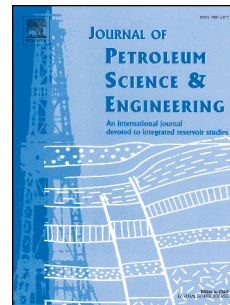


Accepted Manuscript

Slug length for high viscosity oil-gas flow in horizontal pipes: Experiments and prediction

Yahaya D. Baba, Aliyu M. Aliyu, Archibong E. Archibong, Mukhtar Abdulkadir, Liyun Lao, Hoi Yeung



PII: S0920-4105(18)30098-6

DOI: [10.1016/j.petrol.2018.02.003](https://doi.org/10.1016/j.petrol.2018.02.003)

Reference: PETROL 4673

To appear in: *Journal of Petroleum Science and Engineering*

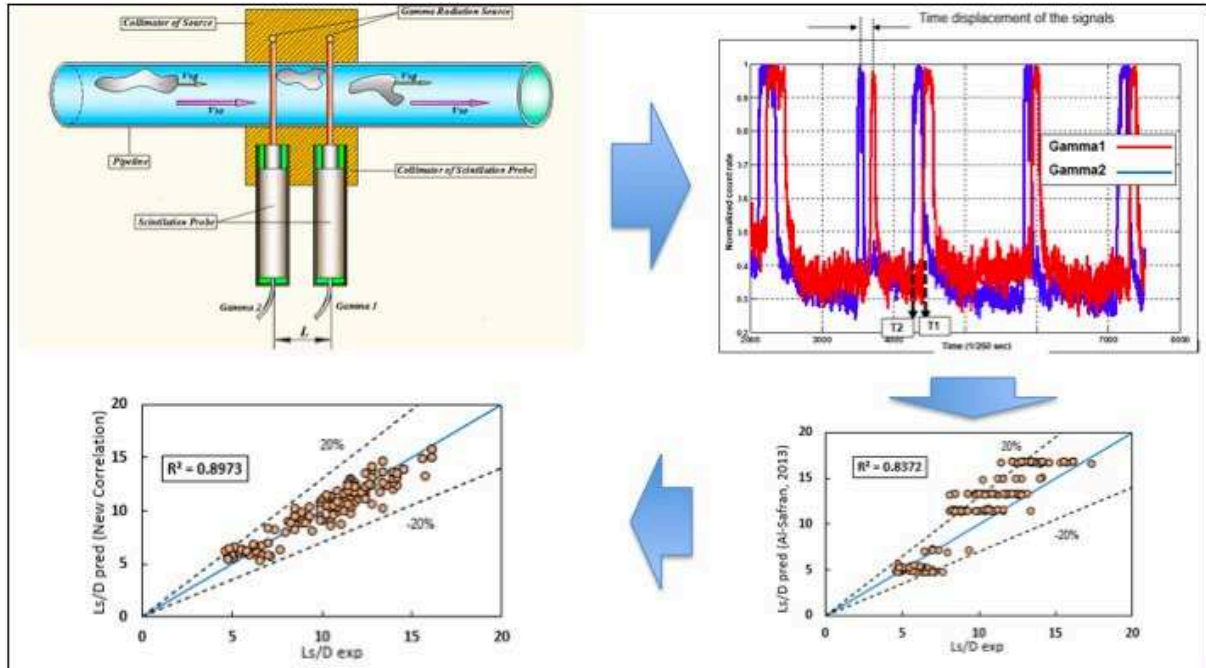
Received Date: 21 September 2017

Revised Date: 30 January 2018

Accepted Date: 1 February 2018

Please cite this article as: Baba, Y.D., Aliyu, A.M., Archibong, A.E., Abdulkadir, M., Lao, L., Yeung, H., Slug length for high viscosity oil-gas flow in horizontal pipes: Experiments and prediction, *Journal of Petroleum Science and Engineering* (2018), doi: 10.1016/j.petrol.2018.02.003.

This is a PDF file of an unedited manuscript that has been accepted for publication. As a service to our customers we are providing this early version of the manuscript. The manuscript will undergo copyediting, typesetting, and review of the resulting proof before it is published in its final form. Please note that during the production process errors may be discovered which could affect the content, and all legal disclaimers that apply to the journal pertain.



1 Slug length for high viscosity oil-gas flow in horizontal pipes: experiments and 2 prediction

3 Yahaya D. Baba^{1,3}, Aliyu M. Aliyu², Archibong E. Archibong^{1,4}, Mukhtar Abdulkadir⁵, Liyun Lao¹ and Hoi
4 Yeung¹

5 ¹*Oil and Gas Engineering Centre, Cranfield University, Bedfordshire MK43 0AL, United Kingdom*

6 ²*School of Mechanical Engineering, Pusan National University, 609-735, Busan, Republic of Korea*

7 ³*Chemical/Petroleum Engineering Department, Afe Babalola University, PMB 5454, Ado Ekiti, Nigeria*

8 ⁴*Department of Mechanical Engineering, Cross River University of Technology, Ekpo Abasi Street, Calabar, Nigeria*

9 ⁵*Department of Chemical Engineering, Federal University of Technology, PMB 65, Minna, Nigeria*

10 Abstract

11 An experimental investigation was carried out on the effects of high liquid viscosities on slug length in a
12 0.0762-m ID horizontal pipe using air-water and air-oil systems with nominal viscosities ranging from
13 1.0-5.5 Pa.s. The measurements of slug length were carried out using two fast sampling gamma
14 densitometers with a sampling frequency of 250 Hz. The results obtained show that liquid viscosity has
15 a significant effect on slug length. An assessment of existing prediction models and correlations in the
16 literature was carried out and statistical analysis against the present data revealed some discrepancies,
17 which can be attributed to fluid properties in particular, low viscous oil data used in their derivation
18 Hence, a new high viscous oil data presented here from which we derive a new slug length correlation
19 was derived using dimensional analysis. The proposed correlation will improve prediction of slug length
20 as well as provide a closure relationship for use in flow simulations involving heavy oil. This is important
21 since most current fields produce highly viscous oil with some reaching 10 Pa.s.

22 **Keywords:** High viscosity oil, gamma densitometer, slug length, translational velocity, two phase flow.

23 1 Introduction

24 1.1 Background

25 The simultaneous flow of gas and liquid in pipelines occurs in many industrial applications which
26 includes the production and transportation of oil and gas from wells. Slug flow is acknowledged as one
27 of the most commonly observed flow patterns for horizontal and near horizontal pipes in operation. This
28 flow pattern is characterized by the intermittent flow of liquid slugs through the whole cross-sectional
29 area of the pipe separated by elongated gas bubbles. A combination of the liquid slugs and the
30 elongated gas bubbles form what is called a slug unit schematically shown in Fig.1. On account of their
31 practical relevance, intermittent flows have lately been investigated both theoretically and
32 experimentally with more emphasis laid on conventional resources (i.e. air-light oil and air-water
33 systems).

34 With the rapid depletion of conventional oil reserves (i.e. those of low to medium viscosity) due to
35 increased energy demands, heavy oil has become a major constituent of unconventional fossil fuel
36 resources. Other unconventional oil sources are tar sands, bitumen, tight gas, coalbed methane (CBM),
37 shale gas, and methane hydrates and together, they constitute a major part of overall global oil
38 resources as illustrated in Figure 2. Conventional crude oil accounts for only 22% of current known
39 reserves. Therefore, it is of utmost importance to study the behaviour and characteristics of highly
40 viscous oils especially their multiphase flow characteristics since they are produced along with water,
41 gas, and other production fluids.

42 **Figure 1: Slug Flow Geometry** (Baba, 2016)

43 **Figure 2: Global oil reserves -conventional versus unconventional resources** (Prestine, 2016)

44 The literature is replete with studies (Ouyang and Aziz, 2000; Santim et al., 2017; Thaker and Banerjee,
45 2015; Abdul-Majeed, 1996, 2000) focusing on air-water two-phase flows. A handful of these studies
46 (Abdulkadir et al., 2016; Al-Safran et al., 2015; Al-Safran, 2009a) address mainly the flow behaviour of
47 medium viscosity liquids (i.e. viscosity < 1 Pa.s). However, there is a severe dearth of studies and data
48 addressing high viscosity oils (i.e. viscosity > 1 Pa.s). We briefly review some of some these studies in
49 Table 1.

50 **Table 1: Summary of experimental studies high viscosity oil-gas flow**

51
52 Pioneering research work was conducted by Weisman et al., (1979) on the effects of fluid properties on
53 two phase flow pattern transition. The investigation was carried out in a 6.1-m long horizontal pipe with
54 internal diameter of 0.012 -0.05-m. Air and water-glycerol mixtures with liquid viscosity range of 0.075-
55 0.150 Pa.s were used as the test fluids. It was concluded that the effects of liquid viscosity on the
56 observed flow pattern transitions were negligible.

57 Andritsos et al., (1989) experimentally studied the effects of liquid viscosity on gas-liquid slug flow
58 initiation in 0.0252-m and 0.0953-m ID horizontal pipes. A mechanism for viscous liquids was proposed
59 noting that that slugs arise from small-wavelength Kelvin-Helmholtz (KH) waves. The proposed
60 mechanism was reported to have shown a good agreement with experimental results.

61 Contrary to the findings of (Weisman et al., 1979), (Nadler and Mewes, 1995) conducted an
62 experimental investigation in a 0.059-m ID horizontal pipe to study the effects of liquid viscosity on the
63 phase distribution of slug flow. They noted that the average liquid holdup within the slug unit and the
64 elongated bubble region increases with increase in liquid viscosity. The viscosity range for their

65 experimental study was from 0.014 - 0.037 Pa·s with the other fluid physical properties being kept
66 constant.

67 Gokcal (2006, 2008) studied the effects high liquid viscosities on two phase flow slug features; slug
68 translational velocities, drift velocity, slug length and slug frequency. His investigation was conducted in
69 a 0.0508-m ID horizontal flow loop of 19-m long for which oil viscosity ranging from 0.18-0.587 Pa·s and
70 air were used as experimental test fluids. New closure relationships for the prediction of the slug flow
71 features taking into account viscosity effects were proposed. Using the same test facility and
72 experimental flow conditions, further work on two phase slug flow in high viscosity liquids was
73 conducted by Al-Safran, (2009b, 2009a) and (Kora et al., 2011). While Al-Safran, (2009b and 2009a)
74 developed new correlations for the prediction of slug liquid holdup and slug frequency, Kora et al. (2011)
75 proposed a correlation from dimensional analysis for the prediction of slug liquid holdup in horizontal
76 pipe.

77 Additional works on high viscous liquids in horizontal pipes were conducted by (Foletti et al., 2011; and
78 Farsetti et al., 2014). While (Folettiet al.(2011) experiment were conducted using oil viscosity of 0.896
79 Pa·s in a 0.022-m ID, Farsetti et al. (2014) used an inclinable rig with 0.028-m ID using oil viscosity of
80 0.9 Pa·s. Both studies presented new data-sets on high-viscosity oil multiphase pipe flows which were
81 compared with those from several empirical and theoretical models. The results of comparison were
82 found to exhibit some discrepancies.

83 More recently, experiments were carried out using relatively high liquid viscosity ranging from 0.07 – 7.0
84 Pa·s by (Zhao et al., 2015; Zhao, 2014) and (Archibong, 2015). Their studies were conducted in both
85 0.0762-m ID horizontal pipe and 0.025-m ID inclinable test facility. Based on their investigation, a
86 dominant intermittent flow region as viscosity increases was observed. While Zhao (2014) developed a
87 correlation for the prediction of slug frequency, Archibong (2015) developed correlations for the
88 prediction of slug frequencies, slug liquid holdup and distribution parameter C_o .

89 The most intrinsic and significant parameters associated with slug flow pattern are the gas and liquid
90 phase distribution, gas bubble and liquid transit frequency and size (i.e. slug length), the velocity of
91 liquid and its fluctuating components, the turbulent transport characteristics of interfacial mass and
92 energy. However, slug length is the most critical slug flow characteristics needed for proper design and
93 safe operation. For example, average slug length is important and preferred (over slug frequency) as
94 an input parameter in mechanistic models to predict liquid holdup and pressure gradient. Furthermore,
95 long slugs often cause operational problems such as flooding of downstream facilities, severe pipe

96 erosion and corrosion, pipeline structural instability, as well as production loss and poor reservoir
97 management due to unpredictable wellhead pressures.

98 It has been reported by (Cook and Behnia, 2000) that slug length characterised by intermittency and
99 irregularity are significant for two reasons. The first been its need as a closure relation for the
100 calculations of liquid holdup and pressure drop by existing mechanistic models such as those of (Dukler
101 and Hubbard, 1975; Taitel and Barnea, 1990). Secondly and most importantly, the statistical distribution
102 of slug length is needed by a pipeline designer for the design of slug catcher and top side processing
103 equipment. A number of researchers (Romero et al., 2012; Xin et al., 2006; Barnea and Taitel, 1993;
104 Heywood and Richardson, 1978) have reported that liquid slug lengths are constant for over a wide
105 range of mixture velocities for in horizontal pipelines. A summary of measured slug lengths by different
106 researchers is presented Table 2 below.

107 **Table 2: Summary of measured slug length by some researchers**

108 Considerable number of models have been developed for the prediction of slug length from
109 different experimental data source, ranging from simple correlations like those proposed by (Brill et al.,
110 1981; Norris, 1982; Scott et al., 1989; Gordon and Fairhurst, 1987; Losi et al., 2016 and Al-safran et al.,
111 2011) to more intricate ones like that by (Wang, 2012). Slug length as estimated by the existing
112 prediction correlations as presented in Table 3 below are expressed by a limited number of flow
113 parameters such as pipe diameter and mixture velocity. However, recent investigations as carried out
114 by (Zhao, 2014; Baba, 2016; Archibong, 2015; Gokcal, 2006; Al-Safran et al., 2015) have shown that
115 the pipe length and diameter, densities and most importantly the viscosities of the liquid phase
116 considerably influence slug flow characteristics. liquid viscosity effects of on slug length have been
117 investigated by (Al-safran et al., 2011; Wang, 2012; Gokcal, 2008 and Losi et al., 2016). All these
118 authors have unanimously concluded that slug length has significant dependency on the liquid viscosity
119 and decreases with increase in liquid viscosity. In addition, these studies are however all limited to
120 viscosity range less than 1.0 Pa s and were conducted in smaller diameter pipelines making it
121 imperative for further investigation.

122 The present study provides new experimental dataset for high viscosity oil-gas two-phase flow for
123 oil viscosity ranging from 1.0 – 5.5 Pa. s. This compliments and extends the viscosity range of existing
124 works (as highlighted in Table 1). Furthermore, we propose a new closure relationship for the prediction
125 of slug length in horizontal pipe. To achieve this, data collected from the Heavy Oil 3-inch Test Facility
126 of the Oil & Gas Engineering Centre, Cranfield University and the published data of (Gokcal,
127 2008). Viscosities ranging between 0.2 and 0.6 Pa.s were utilized. These will significantly contribute to

128 the literature and data on heavy oil as well as provide a new phenomenological based closure
 129 relationship for highly viscous oil flow simulations. Additionally, more and more companies are
 130 extracting from more unconventional reserves and the information on slug length will help to design
 131 processing and transport facilities.

132 **Table 3: Summary of existing correlations in the literature for slug length**

133 **1.2 Slug Flow evolution and initiation criteria**

134 Slug flow is generally classified as hydrodynamic slugging or terrain slugging (severe slugging).
 135 For horizontal or nearly horizontal pipes, though slugs can be generated due to pigging and ramping up, it
 136 is generally accepted that the onset of slugging is caused by two mechanisms; the natural growth of
 137 interfacial instabilities of gas liquid interface of stratified flow (*i.e. Kelvin-Helmholtz Mechanism*) and/or
 138 the accumulation of liquid at valleys of hilly terrain-induced pipelines characterized with sections of
 139 different inclinations, widely known as *terrain slugging*. (Lin and Hanratty, 1987 and Woods et al.,
 140 2006) have also noted wave coalescence at high gas flow rates in horizontal pipes as an important
 141 mechanism in the formation of slug. Taiteland Dukler.(1976) reported that *Kelvin Helmholtz* instability
 142 drives a continuous growth of a small-amplitude long wave into a fully formed slug.

143 A number of researchers have reported the mechanisms connected with slug initiation and the
 144 criteria necessary for the transition of stratified to slug flow ranging from very comprehensive
 145 investigations such as the works of (Taitel and Dukler, 1976; Kordyban and Ranov, 1970; Wallis and
 146 Dodson, 1973; Ujang et al., 2006 and Lin and Hanratty, 1986) to preliminary work like (Dinaryantoa et
 147 al., 2017; Thaker and Banerjee, 2015). A summary of slugging criteria based on the instability analysis
 148 as reported by these researchers is presented in Table 4. However, it is important to note that the
 149 above mentioned slug initiation mechanism from stratified flow have not been validated with high
 150 viscosity liquid (*i.e. viscosity > 0.6 Pa.s*). Zhao (2014), Archibong (2015) and Baba (2016) etc. reported
 151 that no stratified flow in their investigations.

152 **Table 4: Summary of existing models for onset slugging criterion**

154 **1.3 Physical descriptions of the effect of high viscosity**

155 Two important concepts in slug flows are the shedding rate and pick-up rates. On the basis of shedding
 156 and “pick-up” processes, slug flow can be classified into three. Firstly, when the pick-up rate is larger
 157 than the rate of shedding Under such conditions, the resulting slug experiences continuous growth.
 158 Secondly, when the rate of “pick-up” rate is equal to the rate of shedding, the resultant slug becomes

159 fully developed as such the slug length stabilises. However, when the rate of pick-up is less than that of
 160 the shedding rate, the slug under this condition dissipates. This third condition better explains the
 161 characteristics of slug length for very viscous liquids in which shedding exceeds pick-up. A reason for
 162 this occurrence could be the increased forces of cohesion as viscosity increases. To gain insight on
 163 the interaction between the film and the slug front, A physical model for minimum slug length was
 164 developed by (Dukler and Hubbard, 1975) based on the interaction between the film and slug front
 165 simulated in a conduit flow into a large reservoir as illustrated in Fig. 3(a). With the separation of liquid
 166 from the film to the slug front, a recirculation process is achieved. This is formed between the
 167 separation point and a reattachment point also known as the slug mixing zone. The author noted that
 168 the minimum stable slug length in horizontal pipes were $20D$ though, their experimental data showed
 169 slug lengths were in the range of $20-40D$.

170 According to researchers such as (Barnea and Brauner, 1985 and Taitel et al., 1980), a minimum slug
 171 length of $32D$ was obtained from experimental investigation in a horizontal test facility. Two
 172 hydrodynamic parameters according to their model can be deduced to control minimum stable slug
 173 length; the film height and the length of the slug-mixing zone. The effects of liquid viscosity is observed
 174 to affect both parameters as noted by (Al-safran et al., 2013). The author proposed a physical model for
 175 high-viscous-liquid slug as illustrated in Fig. 3(b) in which the height of the film in front of the slug is
 176 thick, suggesting a shorter mixing region and a reattachment distance resulting in shortened slug length
 177 to achieve a fully developed velocity profile.

178 (a)
 179
 180 (b)

181 Figure 3: (a) Physical model minimum slug length in light oil, (Dukler and Hubbard, 1975) (b) physical model minimum slug
 182 length in high viscosity oil, (Al-safran et al., 2013)

183

184 2 Experimental Setup

185 2.1 Test facility description and measurement procedure

186 The experimental setup used for this investigation as shown in the schematics presented in Fig. 4 is
 187 located at the Oil and Gas Engineering Centre Laboratory of Cranfield University. The experimental
 188 flow facility is comprised of the following core sections: the fluid (oil, air and water) handling section, test
 189 measurement/observation section and the instrumentation and data acquisition section. The multiphase

190 flow test facility consists of a 0.0762-m-ID horizontal pipe built using transparent Perspex pipe with an
191 L/D ratio of 223. Researchers like (Baba, 2016; Baba et al., 2017; Archibong, 2015; Okezue, 2013 and
192 Zhao, 2014;) have previously used this facility for related study.

193 2.1.1 Fluid handling section

194 Mineral oil (i.e. CYL680) used as the liquid phase is stored in a steel tank of 2-m³ capacity. It is fed into
195 the main test line through a T-junction (See Fig. 5) using a Progressive Cavity Pump (PCP). Metering of
196 the oil flow rate is done using a commercial Coriolis flow meter with an accuracy of $\pm 0.035\%$ at the
197 inlet. Prior to an experiment, a recirculation of the oil in the tank is done via a by-pass aimed towards
198 achieving a uniform oil viscosity. A refrigerated bath circulator manufactured by Thermal Fisher is used
199 for regulating the temperature of the oil. The temperature range of the circulator is from 0 to +50 °C,
200 with an accuracy of ± 0.01 °C., The oil contained in the tank is either cooled or heated to a desired
201 temperature over a period of time by virtue of changing the temperature of the glycol and hence
202 viscosity of the liquid contained in the tank. It is worth noting that though the mineral oil (CYL680) used for
203 this investigation were specified by manufacturers, there was need to validate their claims before commencing
204 experimental runs. The viscosity of the oil was measured in the laboratory and the result compared well with
205 manufacturer's specifications data as presented in Fig. 6.

206

207 **Figure 4: Schematic of experimental test facility**

208

209 **Figure 5: Pictorial view of test facility injection point.**

210

211 **Figure 6: Comparison of measured viscosity and manufacturer's data**

212

213

214 A 2.5-m³ cylindrical tank is used for storage of water at room temperature supplied from a tap in the
215 laboratory. A variable speed progressive cavity pump (PCP) with maximum capacity of 2.1 m³/hr and a
216 maximum discharge pressure of 10 barg is used for pumping the water into the 3-inch test facility. The
217 rate of water flow is metered using an electromagnetic flow meter with a range of 0–21 m³/hr.

218 Air is used as the gas phase was supplied from a screw compressor with a maximum supply capacity of
219 400 m³/hr. In order to avoid pulsating supply of air to the test facility, the air from the compressor is first
220 discharged into a 2.5-m³ air tank before delivery to the test line where it is regulated to about 7 barg.
221 The flow rates of air were metered using two flow meters: 0.5-inch vortex flowmeter and 1.5-inch vortex
flow meter, ranging from 0–20 and 10–130 m³/h respectively. It is filtered then injected into the main
test line using a 2-inch steel pipe about 150 pipe diameters upstream of the test facility's observation
section as shown in Fig. 5.

222 **2.1.2 Measurement and observation section**

223 The test measurement/observation section is located 14-m downstream from the test fluid inlet pipe.
224 The mixture of the two phase flow (i.e. oil and gas) is achieved at the T-junction upon injection through
225 V4 and V6 as shown in Fig. 5. This is the point where the multiphase flow starts to develop.

226 **2.1.3 Instrumentation and data acquisition section**

227 The separator, gamma densitometer (described in details in 2.3 below) and the heater/chillers (earlier
228 described in 2.1.1) are the three main unit operations equipment used in the for this investigation. The
229 separator positioned at the end of the pipeline is a rectangular shaped steel tank with viewing windows
230 is used for the collection and separation of the multiphase fluid into phases. The test fluids are allowed
231 to settle for 48 hours. Air is vented to the atmosphere, Oil and water are transferred to their respective
232 storage tanks and reused.

233 The temperature of the test fluids is measured using a J-type thermal couples with an accuracy of
234 $\pm 0.1^{\circ}\text{C}$ placed at different locations along the test line. while differential pressure transducers installed
235 at 4-m and 13-m downstream of the test line were used for pressure measurement. Acquired data from
236 the temperature sensors, flowmeters and differential pressure transducers are saved to a Desktop
237 Computer using a LabVIEW-based system. This system comprised of a National Instruments (NI) USB-
238 6210 connector board interface that output signals from the instrumentation using BNC coaxial cables
239 connected the desktop computer.

240 **2.2 Test Matrix**

241 A summary of the experimental test fluid properties and the adopted test matrix used for this
242 investigation are presented in Table 5. The uncertainties in the measurement of superficial gas and
243 liquid velocities, liquid hold and viscosities as presented in Table 6 were obtained based on
244 manufacturers' specification of flow meters, viscometer, and gamma sensor. This is in agreement with
245 values obtained upon carrying out repeatability tests to ascertain accuracy of the values.

246 **Table 5: Experimental test matrix and fluid properties**

247

248 **Table 6: Uncertainties in measurements**

249

250 2.3 Instrumentation and calibration

251 A fixed single beam gamma densitometer as illustrated in Fig. 7 was used for the measurement of the
 252 phase fraction. This is comprised of a single energy source block and a Sodium Iodide (NaI) scintillation
 253 radiation detector. A 5.5 Gigabecquerel (GBq) Caesium-137 radioisotope is contained in the source
 254 block housed within a lead radiation protection shield and further encased in stainless steel. The
 255 Caesium-137 radioisotope in the instrumentation is a dual-energy source emitting gamma rays in two
 256 broad photon energy levels; the gamma radiation transmitted is the source of the 662-keV high-energy
 257 level while scattered gamma radiation is the source of the lower energy level range of 100 keV–300
 258 keV. At a sampling rate of 250 Hz, the sodium iodide (NaI) scintillation radiation detector was used to
 259 measure two separate sets of gamma attenuation data for the high and low energy levels. A proprietary
 260 Data Acquisition System (DAS) was used for voltage signal acquisition and a ICP i-7188 programmable
 261 logic controller which is used to convert the raw voltage to gamma counts signals (i.e. counts are the
 262 remainder of the attenuation signals after absorption by the media it passes through).

264 **Figure 7: Pictorial representation of gamma ray densitometer used as instrumentation**

265
 266 Eq. (1) below represents the Beer-Lambert equation used for linear attenuation coefficients
 267 computation and hence, the liquid holdup. For an empty pipe, the gamma radiation beam's intensity
 268 remains unchanged inside the pipe because is virtually zero in comparison.

$$\lambda_L = \left[\frac{\ln \left(\frac{I_M}{I_A} \right)}{\ln \left(\frac{I_L}{I_A} \right)} \right] \quad (1)$$

269 Where

270 I_M = average gamma count obtained from liquid-gas mixture in the pipeline

271 I_A = average calibration gamma count obtained for empty pipe (i.e. 100% Air)

272 I_L = average calibration gamma count obtained for pipe containing pure liquid

273 λ_L = Liquid Hold Up

274 A typical plot from of the Gamma Densitometer liquid holdup time series exhibits an intermittent
 275 behaviour for slug flow as presented in Fig. 8 characterized by crests and troughs. While the trough
 276 region is suggestive of the passage of liquid slugs, the crest regions are indicative of the slug film
 277 region. The holdup time traces obtained from two gamma densitometers positioned at 103D and 124D

278 (see Fig. 9) downstream of the oil injection point were used for the slug translational velocity data
 279 collection. This is achieved by carrying out a cross-correlation using the MATLAB signal processing
 280 toolbox.

281

282 **Figure 8: A typical gamma densitometer time series liquid holdup plot for dual Gamma Sensor**

283

284 **Figure 9: Diagrammatic representation of the Gamma Source installed on the test facility.**

285

286 From Figure, if the distance between the two gamma densitometers is represented by Δl_{Gamma} and
 287 assuming the arrival time of the slug front at first and second gamma densitometers are denoted by T_1
 288 and T_2 respectively, obtained by virtue of the passage of a slug body through the cross sectional area
 289 of the pipe where the gamma detectors are located. Then the translational velocity is given by;

$$V_T = \frac{\Delta l_{Gamma}}{T_1 - T_2} \quad (2)$$

290 Slug length is obtained by multiplying the time difference between the period of passage of the slug
 291 body through the two gamma densitometer and the translational velocity of the slug obtained from Eq.
 292 (2). Therefore slug length L_S ,

$$L_S = V_T \times \tau \quad (3)$$

293 where τ is the time or temporal lag between the signals registered by the two densitometers. It is
 294 obtained by cross-correlation and explained in section 2.5. Owing to the randomness in the gamma
 295 photon emissions obtained from the source (i.e. caesium-137), there was a need to determine the
 296 statistical uncertainty in the gamma beam measurements. The uncertainty in this case is inversely
 297 proportional to the measurement time adopted for experimental runs This is described by the equation:

$$SU = \frac{1}{S\sqrt{N_{Count}}} \quad (4)$$

298 where SU is the statistical uncertainty. It depends on the sensitivity (S) of the densitometer as well as
 299 that of the gamma attenuation data (N_{Count}) size measured for the multiphase flow (i.e. oil-gas)
 300 mixture over a certain period of time. Therefore, sensitivity is the relative difference between the
 301 response of the gamma densitometer to pure liquid and to pure gas:

$$S = \frac{I_G - I_L}{0.5(I_G + I_L)} \quad (5)$$

302 Where I_G and I_L are respectively the mean gamma count values obtained when the gamma beam
 303 densitometer was calibrated using 100% air and 100% oil. As was reported by Okezue (2013), the
 304 current gamma densitometer attenuation data recordings gave an average statistical uncertainty of
 305 1.70%. Readings were taken at a mean measurement time of 70s per experimental run. Other sources
 306 of error in the measurements are systematic error in the Sodium Iodide (NaI) scintillation radiation
 307 detector and errors arising from the dynamic fluctuation of the gas–liquid two-phase flow field in the
 308 cross-sectional area of the measurement pipe section. It is estimated that the sum total of the error
 309 sources mentioned result in a maximum of 5% uncertainty in the slug lengths measured by the gamma
 310 densitometer. In view of this, error bars have been added to relevant figures to account for these effects.

311 **2.4 Data Processing**

312 The randomness characteristics feature of gamma radiation distorts the output signal, thus providing an
 313 inferior signal quality on the receiving end and hence, the need to filter the raw output signal in order to
 314 improve data quality. For the purpose of this study, the analysis was conducted using MATLAB to filter
 315 the output signals from the gamma densitometer. The “smooth” function was used. It utilizes a moving
 316 average filter (average of 8) aimed towards noise reduction. Presented in Figs 10(a) and (b) are typical
 317 example of raw and filtered signal output from the gamma densitometer.

318

319 **Figure 10: (a) Raw signal output from gamma photon counts. (b) Sample of a filtered signal output.**

320

321 **2.5 Cross-correlation Procedure**

322 Cross-correlation is a standard method which measures the degree to which two signals correlate with
 323 one another with respect to the time displacement that exist between them. The cross-correlation for
 324 similar and identical signal tends towards unity or unity and if they are dissimilar, the cross-correlation
 325 tends to zero or even zero. Assuming two-time series, $X(t_n)$ and $Y(t_n)$, where $n=0, 1, 2, 3, \dots, N-1$,
 326 then the cross correlation coefficient is defined as;

$$R_{xy}(\tau) = \frac{C_{xy}(\tau)}{\sqrt{C_y(0)C_y(0)}} \quad (6)$$

$$C_{xy}(\tau) = \frac{1}{N - \tau} \sum_{n=1}^{N-\tau} X(t_n) Y(\tau + t_n), \quad (7)$$

327 Where τ is the temporal lag.

328 The filtered signal output from both gamma densitometers are then used for performing a cross-
 329 correlation. It is worth noting that a better correlation is achieved if the output of the cross correlation
 330 function result tends towards “1” and no correlation if it tends towards “0”. Fig. 11 shows a clear cross-
 331 correlation between the two-time series signal output.

332

333 **Figure 11: Cross-Correlation results between Gamma 1 and Gamma 2.**

334

335 **3 Results and discussion**

336 **3.1 Experiments with air and water**

337 Initial experiments were carried out using air and water ($\mu = 0.001$ Pa.s). Since data for air/water
 338 mixtures are widely available, comparing our slug lengths with those in those in the literature will ensure
 339 the reliability of experimental data collected from the experimental rig. Fig. 12(a) shows the slug lengths
 340 we obtained plotted as a function of mixture velocity. It indicates that the measured slug length is
 341 approximately 24-36D with a mean length of 30.6D. This agrees with the work of Pan (2010) who
 342 reported a mean length of 30D with an approximate length of 20-40D for air-water experiments in a
 343 0.0762 m ID horizontal pipe. His investigation further revealed a mean length of 24D for 0.004 Pa.s oil-
 344 air experiments. It is worth noting that experimental observations by previous authors (Nicholson et al.,
 345 1978; Barnea and Brauner, 1985; Fabre and Line, 1992; Dukler and Hubbard, 1975) for air–water
 346 systems in upward vertical and horizontal flows suggest that the average stable liquid slug length is
 347 largely insensitive to the gas and liquid flow rates and depends mainly on the pipe diameter. Previous
 348 authors also reported measured slug lengths within the range of 15–40D with an average slug length
 349 of 30D. We plotted the distribution of slug lengths obtained at $V_{sg} = 0.3 - 7$ m/s and $V_{sl} = 0.2 -$
 350 0.4 m/s in Fig. 12(b) and as can be seen, a lognormal curve describes the experimental data quite
 351 well. This is consistent with the findings of (Nydal et al., 1992) who also reported that their
 352 experimental slug lengths were log-normally distributed and right-skewed.

353 **Figure 12: (a) Measured slug length as a function of mixture velocity (b) Slug length distribution and log-normal fit for flow**
 354 **conditions investigated ($V_{sg}=0.3-7$ m/s and $V_{sl}=0.2-0.4$ m/s)**

3.2 Flow Pattern Characterization for High Viscosity Oil Gas Flows

Flow pattern characterization for this investigation was achieved by using High Speed Video camera. Presented in Table 7 are the flow patterns observed for this study. There are; plug flow, slug flow, pseudo slug and wavy annular flow patterns. Plug flow and slug flow are both termed as “intermittent flow”. To begin with, the intermittent flow was observed to dominate the entire flow regime and this is line with previous findings (Gokcal, 2006, 2008; Zhao, 2014; Archibong, 2015 and Baba et al., 2017). It is a flow pattern characterised by an intermittency i.e. the alternation of series of slugs (plugs) largely separated by gas pockets. The distinctive parameter of slug flow pattern from plug flow, is the presence of pronounced gas entrainments in the former than the latter. The intermittent flow pattern is closely followed by a transition flow pattern termed as “pseudo slug” (i.e. transition from intermittent to wavy-annular flow pattern). It is mostly characterised by large energetic travelling waves. Further increase in the gas superficial velocity results in the formation of wavy-annular flow pattern characterised by high gas momentum which sweeps most of the liquid phase around the pipe walls with a rolling wave at the interface. It is worth noting that a temporary emulsion formation was observed during the course of this investigation at relatively very high superficial gas velocities. This occurrence is due to the agitation of the gas phase (i.e. its tendency in displacing the liquid phase leads to the gas to be entrained in the liquid phase) and viscosity of the liquid phase. In addition, the high viscosity property of the liquid makes it difficult for the entrained gas to escape easily and this explains the higher entrainment characteristic feature of slug formation in highly viscous liquid.

Table 7: Snapshots of observed flow patterns

3.3 Slug Length for High Viscosity Liquid

Fig. 13(a) shows the measured mean slug length plotted as a function of gas superficial velocity for oil superficial velocities (0.06~0.3 m/s) for varying oil viscosities. The plot shows a strong dependence of slug length on liquid viscosity as slug body length decreased with increase in liquid viscosity. The measured length of slug was in the range of 4-9D with an average length of 6D as against 8-14D, 15-40D, 15-27D, 12-30D, 10-34D and 15-27D ranges obtained respectively by (Al-safran et al., 2011; Dukler and Hubbard, 1975; Nicholson et al., 1978; Nydal et al., 1992; He, 2002 and Xin et al., 2006). A comparison of mean slug length plotted as a function of mixture velocity for this study and (Al-safran et al., 2012) is presented in Fig. 13(b). Most researchers (Hernandez, 2007; Pan, 2010; Gokcal, 2008) unanimously reported that slug length are generally insensitive to flow conditions (i.e. changes in gas

387 superficial velocity and liquid superficial velocity). The trend observed corroborates the findings of
 388 (Hernandez, 2007; Pan, 2010; Gokcal, 2008) as can be seen illustrated in Fig.15 where there is an
 389 irregular nature of the data relative to the uncertainties of time of passage of the slug body.

390

391 **Figure 13: (a) Measured slug length versus superficial gas velocity for different superficial liquid velocity $V_{sl}=0.06-0.3\text{m/s}$. (b)**
 392 **Mean Slug Length as a Function of Mixture Velocity. Error bars were calculated from the uncertainty equation (i.e. Eq. 12) given**
 393 **in Appendix.**

394

395 Liquid slug length data are generally described by positively skewed distributions (i.e. log-normal
 396 distribution) according to (Van-Hout et al., 2001; Gokcal, 2008; Nydal et al., 1992). In view of this, Easy
 397 Fit software 3.0 was used to determine the mean and standard deviation of the Log-Normal distribution.
 398 Presented in Fig. 14 is the comparison between experimental result and Log-Normal distribution which
 399 exhibited a good match.

400

Figure 14: Comparison of experimental result for slug length and Log-Normal distribution.

401

402 **4 Relationship for Slug Length**

403 Slug length as deduced from our experimental observations and published works is a function of
 404 density, velocity, pipe diameter and fluid properties (i.e. Eq. 8).

$$\frac{L_s}{D} = f(\rho_m, V_m, D, \mu_L, g) \quad (8)$$

405 Carrying out dimensional analysis by applying the Buckingham Pi-theorem yielded the following
 406 dimensionless groups – the mixture Reynolds number, mixture Froude number and viscosity number:

$$\frac{L_s}{D} = f(Re_m, Fr_m, N_\mu) \quad (9)$$

407 Where Re is the Reynolds number defined as $\frac{\rho_m V_m D}{\mu_L}$. It's use as a candidate for correlation is
 408 consistent as it captures inertia changes prompted by changes in fluid superficial velocities relative to
 409 viscous forces. In addition, the Reynolds number provides information necessary for categorising the
 410 flow of the two-phase mixture into the laminar or turbulent flow regions. It should be noted that μ_L was
 411 used because $\mu_L \gg \mu_g$ thus making μ_g negligible. The Froude number represented by $\frac{V_m}{\sqrt{gD}}$ is a
 412 dimensionless number which is used in hydrodynamics studies to indicate the influence of gravity on
 413 fluid motion. It is the ratio of inertial forces of pressure driven gas/liquid flow to the opposing

414 gravitational force. Finally, N_μ is the viscosity number, which is defined as $\frac{\mu_L}{\rho_m g^{1/2} D^{3/2}}$ captures the
 415 overriding influence of oil viscosity on slug length. Assuming the nature of the functional dependency of
 416 slug length on the dimensional groups is in the form of a power law relationship, we can express Eq. (9)
 417 as follows:

$$\frac{L_s}{D} = \alpha Fr_m^\beta N_\mu^\gamma Re_m^\delta \quad (10)$$

418 Where the factor α and the indices β , γ , and δ are constants to be determined upon correlating with
 419 the acquired experimental dataset using multiple non-linear regression. Therefore, the new correlation
 420 for new mean slug length for high viscosity oil-gas flow is proposed as:

$$\frac{L_s}{D} = 3.35 Fr_m^{0.03} N_\mu^{-0.2} Re_m^{0.1} \quad (11)$$

421 Eq. 10 was obtained using the current data and those of (Gokcal, 2008). Notable in the equation is the
 422 relative insensitivity of dimensionless slug length L_s/D to the mixture Froude and Reynolds numbers.
 423 This is consistent with the work of Al-Safran et al. (2013) in which their slug length correlation for
 424 medium viscosity oils was only dependent on the dimensionless viscosity number N_μ . In their
 425 proposed correlation, N_μ was raised to the exponent -0.321 compared with the -0.2 in Eq. 10.
 426 However, slug length decreases monotonically with increase in oil viscosity meaning that a point could
 427 be reached where further increasing the viscosity will have little or no effect on the length of the liquid
 428 slug.

429 4.1 Validation of proposed correlation

430 Performance of the proposed slug length prediction model was examined against selected slug length
 431 correlations in the literature. Correlations whose predictive performance were evaluated include; (Brill et
 432 al., 1981; Norris, 1982; Scott et al., 1989; Wang, 2012; Al-safran et al., 2013). Results presented in
 433 Table 15 below shows that all the existing prediction correlations found in the literature over-predict the
 434 average slug length with huge discrepancies. The correlations of (Brill et al., 1981; Norris, 1982; Scott
 435 et al., 1989) over predict obtained experimental data with very wide error margin. This can be attributed
 436 to the fact that there were developed using conventional fluids (i.e. low viscosity liquids (<0.01 Pa.s).
 437 Al-safran et al. (2013) unlike Wang, 2012 performed fairly well even though both were developed and
 438 tested using dataset from the same viscosity range. This can be credited to the fluid properties inherent
 439 in Al-safran et al., 2013 as against Wang, 2012. A comparison of experimental measurements against
 440 the best performing predicted models as highlighted in Table 8 is presented in the Figs 15(a)-(c).

441

442

(a)

443

444

(b)

445

446

(c)

447

Figure 15: Cross-plot of predictive model predictions for best performing correlations against experimental measurement (a)

448

Current (b) Al Safran (2013) (c) Brill (1981)

449

Fig. 16 shows simulations carried out using Eq. (9) to predict the effect of oil viscosity and mixture Reynolds number on the slug length. Comparisons were made with the experimental data of Al-Safran et al. (2013) who performed their experiments in a 0.0508-m pipe with oil viscosities of 0.18–0.59 Pa.s. Also, the current data was compared and as can be seen, there is good agreement as all were within the $\pm 20\%$ error margin shown in Fig. 15(a).

454

455

Figure 16: Use of Al-Safran (2013) and current experimental data concerned with oil viscosities ranging from 0.18–6.00 Pa.s to validate Eqn. (9)

456

457

Finally, Table 8 shows the results of statistical analysis carried out on the current data, using the proposed correlation Eq. (9) and those of Brill (1981), Norris (1982), Scott (1989), Wang (2012), and Al-Safran (2013). The statistical parameters $\varepsilon_1 - \varepsilon_6$ in the table are the relative error, average relative error, absolute relative error, standard deviation about the relative error, average actual error, and the standard deviation of the actual error respectively. Their mathematical relationships are defined in the Appendix. These show that the new correlation produced the least value for each of the statistical parameters indicating improved prediction on the previous ones and this is due to the fact that previous correlations were obtained with data at far lower viscosities than those used in our experiments. This underlines the importance of viscosity and its dominance in closure relationship predictions which can have a profound effect on the accuracy of flow simulators for heavy oils. In summary, the comparative analysis reveals the need for a slug length prediction correlation in high viscous pipe flow systems.

468

469

Table 8: Statistical evaluation of surveyed slug length correlations

470

471 5 Conclusion

472 A new set of experimental data for two-phase flow slug length using high-viscosity mineral oil as the
 473 liquid phase and air as the gas phase. The experiments were conducted in a 0.0762 m ID horizontal
 474 pipe using a fast-sampling gamma densitometer) at a frequency of 250Hz. Results show that slug
 475 length decreases with increasing liquid viscosity and is relatively insensitive to changes in the individual
 476 superficial liquid viscosities. However, we find that slug length is very sensitive to changes in liquid
 477 viscosity. The minimum 32D slug length proposed by researchers (Barnea and Brauner, 1985; and
 478 Taitel et al., 1980) for liquid slug length in horizontal pipeline was found to be much shorter once
 479 viscosity exceeds 0.1 Pa.s. For the current viscosity range, 1 – 5.5 Pa.s, the mean slug length was
 480 approximately 6D which is not far from the 10D obtained by Al-Safran et al. (2013) for the range of 0.18
 481 – 0.59 Pa.s. A performance evaluation of existing correlations was carried out against the present data
 482 and wide discrepancies were revealed. This can be attributed to the use of oil data lower than 1 Pa.s to
 483 derive these models. As a result, a new correlation for slug length was obtained using the current data
 484 with the correlation exhibiting a better prediction of the dataset. It will therefore serve as a significant
 485 improvement for the prediction of heavy oil slug length than previous ones based on low viscous oils.

486 6 Acknowledgment

487 The author of this work is grateful to Petroleum Technology Development Fund (PTDF) under the
 488 auspices of the Nigerian Government for funding his Doctoral research programme with the Oil and
 489 Gas Engineering Centre of Cranfield University United Kingdom. The support and kind assistance of
 490 fellow research colleagues at Cranfield University is highly acknowledged.

491 7 Appendix

492 7.1 Error Analysis

493 The uncertainty in determining the slug length is given as a relative error which depends on the relative
 494 errors in the translational velocity and the time lag between the two gamma densitometer readings as
 495 follows:

$$\frac{\delta L_S}{L_S} = \sqrt{\left(\frac{\delta V_T}{V_T}\right)^2 + \left(\frac{\delta \tau}{\tau}\right)^2} \quad (12)$$

496 where δ is the uncertainty in the quantity that follows it. For translational velocity, its uncertainty is
 497 related to the sensitivity S of the gamma readings given in Eq. 5. On the other hand, the uncertainty in

498 τ is fixed by the cross-correlation procedure which is limited by the sampling rate of each densitometer
 499 which in this case is 250 Hz (or $1/250 = 0.004$ s).

500 7.2 Statistical Parameters

501 Six statistical parameters were used to evaluate the performance of predictive correlations relative to
 502 the experimental data acquired. These parameters were also used by several researchers such as
 503 (Gokcal et al., 2009; Al-Safran, 2009a; Kora et al., 2011; Zhao, 2014) and are evaluated based on two
 504 types of errors; actual and relative error defined in Eqs. (15) and (18) respectively. Results are given in
 505 Table 8 and the best performing correlations are those with the least magnitude of the statistical
 506 parameter concerned. They are:

$$\varepsilon_i = \frac{y_{predicted} - y_{measured}}{y_{measured}} * 100 \quad (13)$$

$$\varepsilon_j = y_{predicted} - y_{measured} \quad (14)$$

507 Based on the error margin from estimated actual error and relative error above, six other statistical
 508 parameters are defined from Eqs. (15) to (20)

509 The average relative error is given as:

$$\varepsilon_1 = \frac{1}{N} \sum_{i=1}^N y_i \quad (15)$$

510 The absolute of average relative error is given as:

$$\varepsilon_2 = \frac{1}{N} \sum_{i=1}^N |y_i| \quad (16)$$

511 While standard deviation about the relative error is given by:

$$\varepsilon_3 = \sqrt{\frac{\sum_{i=1}^N (y_i - Y_1)^2}{N - 1}} \quad (17)$$

512 The average actual error

$$\varepsilon_4 = \frac{1}{N} \sum_{j=1}^N y_j \quad (18)$$

513 The absolute of the average actual error is given by

$$\varepsilon_5 = \frac{1}{N} \sum_{i=1}^N |y_j| \quad (19)$$

514 And finally, the standard deviation of actual errors is given by:

$$\varepsilon_6 = \sqrt{\frac{\sum_{j=1}^N (y_j - Y_4)^2}{N - 1}} \quad (20)$$

515 The average relative error ε_1 and the average actual error ε_4 are the agreement between the
 516 predicted and measured parameters. Positive numbers indicate over-estimation of the parameter and
 517 vice versa. Individual error can be either positive or negative, and they can cancel each other, masking
 518 the true performance. The average absolute percentage relative error ε_2 and the average absolute
 519 actual error ε_5 do not have masking effect. However, they indicate how large the error is on the
 520 average. The standard deviation ε_3 and ε_6 indicate the degree of scattering with respect to their
 521 corresponding average errors ε_1 and ε_4 .

522 8 Nomenclature

Symbol	Denotes	Units
<i>A</i>	Area	m^2
<i>C</i>	Constant	
<i>D</i>	Pipe diameter	m
<i>Fr</i>	Froude number	
<i>f_s</i>	Slug Frequency	s^{-1}
<i>g</i>	Acceleration due to gravity	$m \cdot s^{-2}$
<i>L</i>	length	m
<i>h_{G,L}</i>	Height	m
<i>N_μ</i>	Viscosity number	
<i>H_L</i>	Holdup	
<i>H_F</i>	Average film holdup	
<i>H_S</i>	Average slug holdup	
<i>N_f</i>	Inverse viscosity number	
<i>Re</i>	Reynolds number	
<i>St</i>	Strouhal number	
<i>V_M</i>	Mixture Velocity	m/s
<i>L_s</i>	Liquid slug length	m

V_{SG}	Superficial Gas Velocity	m/s
V_{SL}	Superficial Liquid Velocity	m/s
V_T	Translational velocity	m/s
J_{GL}	Non-dimensional gas-liquid relative velocity	
S_i	Wetted perimeter interface	
Greek letter		
μ	Viscosity	Pa.s
λ_L	Liquid holdup	
ρ	Density	kg/m ³
$\Delta\rho$	Density difference	
τ	Shear stress	Pa
α	Void fraction	
ε_{1-6}	Relative error	
Subscripts		
f	Film zone	
g	Gas phase	
l	Liquid phase	
m	Mixture phase	
s	Superficial	
t	Translational	

524 **9 References**

- 525 Abdul-Majeed, G. H. (1996) Liquid holdup in horizontal two-phase gas—liquid flow. *Journal of*
526 *Petroleum Science and Engineering*. [Online] 15 (2–4), 271–280. [online]. Available from:
527 <http://linkinghub.elsevier.com/retrieve/pii/S0920410595000690> (Accessed 21 August 2017).
- 528 Abdulkadir, M., Hernandez–Perez, V., Lowndes, I. S., Azzopardi, B. J., and Sam–Mbomah, E., 2016.
529 “Experimental study of the hydrodynamic behaviour of slug flow in a horizontal pipe”. *Chemical*
530 *Engineering Science* 156, 147-161
- 531 Abdul-Majeed, G. H. (2000) Liquid slug holdup in horizontal and slightly inclined two-phase slug flow.
532 *Journal of Petroleum Science and Engineering*. [Online] 27 (1–2), 27–32. [online]. Available from:
533 <http://www.sciencedirect.com/science/article/pii/S092041059900056X> (Accessed 19 July 2014).
- 534 Al-safran, E. et al. (2011) ‘High Viscosity Liquid Effect on Two-Phase Slug Length in Horizontal Pipes’,
535 in *15th International Conference on Multiphase Production Technology*,. 2011 Cannes, France:
536 BHR Group. pp. 257–276.
- 537 Al-Safran, E. (2009a) Investigation and prediction of slug frequency in gas/liquid horizontal pipe flow.
538 *Journal of Petroleum Science and Engineering*. [Online] 69 (1–2), 143–155. [online]. Available
539 from: <http://www.sciencedirect.com/science/article/pii/S0920410509001788> (Accessed 25 March
540 2014).
- 541 Al-Safran, E. et al. (2015) Prediction of slug liquid holdup in high viscosity liquid and gas two-phase flow
542 in horizontal pipes. *Journal of Petroleum Science and Engineering*. [Online] 133566–575. [online].
543 Available from: <http://www.sciencedirect.com/science/article/pii/S0920410515300450> (Accessed
544 22 August 2015).
- 545 Al-Safran, E. (2009b) Prediction of Slug Liquid Holdup in Horizontal Pipes. *Journal of Energy*
546 *Resources Technology*. [Online] 131 (2), 23001. [online]. Available from:
547 <http://energyresources.asmedigitalcollection.asme.org/article.aspx?articleid=1414905> (Accessed
548 15 April 2014).
- 549 Al-safran, E. M. et al. (2013) Investigation and Prediction of High-Viscosity Liquid Effect on Two-Phase
550 Slug Length in Horizontal Pipelines. *SPE Production & Operations*. [Online] 28 (3), 12–14.
- 551 Andritsos, N. et al. (1989) Effect of Liquid Viscosity on the Stratified-Slug Transition in Horizontal Pipe
552 Flow. *International Journal of Multiphase Flow*. 15 (6), 877–892.
- 553 Archibong-Eso, A. et al. (2015) ‘Viscous liquid-gas flow in horizontal pipelines: Experiments and
554 multiphase flow simulator assessment’, in *BHR Group - 17th International Conference on*
555 *Multiphase Technology 2015*. 2015 p.
- 556 Archibong, A. (2015) *Viscous Multiphase Flow Characteristics in Pipelines*. PhD Thesis thesis. United
557 Kingdom: Cranfield University, United Kingdom.
- 558 Baba, Y. D. (2016) *Experimental Investigation of High Viscous Multiphase Flow in Horizontal Pipelines*.
559 PhD Thesis thesis. Cranfield University.
- 560 Baba, Y. D. et al. (2017) Slug frequency in high viscosity oil-gas two-phase flow : Experiment and
561 prediction. *Flow Measurement and Instrumentation*. [Online] 54 (December 2016), 109–123.
562 [online]. Available from: <http://dx.doi.org/10.1016/j.flowmeasinst.2017.01.002>.
- 563 Barnea, D. & Brauner, N. (1985) Holdup of the liquid slug in two phase intermittent flow. *International*
564 *Journal of Multiphase Flow*. [Online] 11 (1), 43–49. [online]. Available from:
565 <http://www.sciencedirect.com/science/article/pii/0301932285900047> (Accessed 30 December
566 2015).
- 567 Barnea, D. & Taitel, Y. (1993) A model for slug length distribution in gas-liquid slug flow. *International*
568 *Journal of Multiphase Flow*. [Online] 19 (5), 829–838.
- 569 Brill, J. P. et al. (1981) Analysis of Two-Phase Tests in Large-Diameter Flow Lines in Prudhoe Bay
570 Field. *Society of Petroleum Engineers*. [Online] 21 (3), .
- 571 Brito, R. et al. (2014) ‘Experimental study to characterize slug flow for medium oil viscosities in

- 572 horizontal pipes', in *9th North American Conference on Multiphase Technology*. 2014 Banff,
573 Canada: BHR Group. pp. 403–417.
- 574 Cook, M. & Behnia, M. (2000) Slug length prediction in near horizontal gas-liquid intermittent flow.
575 *Chemical Engineering Science*. 55 (11), 2009–2018.
- 576 Dinaryantoa, O. et al. (2017) Experimental investigation on the initiation and flow development of gas-
577 liquid slug two-phase flow in a horizontal pipe. *Experimental Thermal and Fluid Science*. 8193–
578 108.
- 579 Dukler, A. E. & Hubbard, M. G. (1975) A Model for Gas-Liquid Slug Flow in Horizontal and Near
580 Horizontal Tubes. *Industrial & Engineering Chemistry Fundamentals*. [Online] 14 (4), 337–347.
581 [online]. Available from: <http://pubs.acs.org/doi/abs/10.1021/i160056a011>.
- 582 Fabre, J. & Line, A. (1992) Modeling of Two-Phase Slug Flow. *Annual Review of Fluid Mechanics*.
583 [Online] 24 (1), 21–46. [online]. Available from:
584 <http://dx.doi.org/10.1146/annurev.fl.24.010192.000321>.
- 585 Farsetti, S. et al. (2014) Experimental investigation of high viscosity oil–air intermittent flow.
586 *Experimental Thermal and Fluid Science*. [Online] 57285–292. [online]. Available from:
587 <http://www.sciencedirect.com/science/article/pii/S0894177713002847> (Accessed 21 January
588 2015).
- 589 Gokcal, B. (2008) *An Experimental and Theoretical Investigation of Slug Flow for High Oil Viscosity in*
590 *Horizontal Pipes*. PhD Thesis thesis. USA: The University Tulsa, USA.
- 591 Gokcal, B. et al. (2006) 'Effects of High Oil Viscosity on Oil / Gas Flow Behavior in Horizontal Pipes', in
592 *SPE Annual Technical Conference and Exhibition*. [Online]. 2006 San Antonio, Texas, U.S.A.:
593 Society of Petroleum Engineers. p.
- 594 Gokcal, B. (2006) *Effects of High Oil Viscosity on Two-Phase Oil–Gas Flow Behavior in Horizontal*
595 *Pipes*. M.Sc Thesis thesis. University of Tulsa.
- 596 Gokcal, B. et al. (2009) 'Prediction of Slug Frequency for High Viscosity Oils in Horizontal Pipes', in
597 *SPE Annual Technical Conference and Exhibition*. [Online]. 2009 New Orleans, Louisiana, USA:
598 Society of Petroleum Engineers. p.
- 599 Gordon, I. C. & Fairhurst, P. C. (1987) 'Multi-phase Pipeline and Equipment Design for Marginal and
600 Deep Water Field Development', in *3rd International Multiphase Flow Conference*. 1987 The
601 Hague, Netherland: BHR. pp. 1–12.
- 602 Grassi, B. et al. (2011) Experimental investigation on two-phase air / high-viscosity-oil flow in a
603 horizontal pipe. *Chemical Engineering Science*. [Online] 665968–5975.
- 604 He, L. (2002) *An investigation of the characteristics of oilgas two-phase slug flow in horizontal pipes*.
605 Xi'an Jiaotong University.
- 606 Hernandez, P. V. (2007) *Gas-liquid two-phase flow in inclined pipes*. PhD Thesis thesis. University of
607 Nottingham.
- 608 Heywood, N. I. & Richardson, J. F. (1978) Slug flow of air–water mixtures in a horizontal pipe:
609 Determination of liquid holdup by γ -ray absorption. *Chemical Engineering Science*. [Online] 34 (1),
610 17–30. [online]. Available from:
611 <http://www.sciencedirect.com/science/article/pii/000925097985174X> (Accessed 30 August 2015).
- 612 Van Hout, R. et al. (2001) Evolution of statistical parameters of gas–liquid slug flow along vertical pipes.
613 *International Journal of Multiphase Flow*. [Online] 27 (9), 1579–1602. [online]. Available from:
614 <http://www.sciencedirect.com/science/article/pii/S0301932201000167> (Accessed 30 October
615 2015).
- 616 Kora, C. et al. (2011) 'Effects of High Oil Viscosity on Slug Liquid Holdup in Horizontal Pipes', in
617 *Canadian Unconventional Resources Conference*. [Online]. 2011 Alberta, Canada: Society of
618 Petroleum Engineers. p.
- 619 Kordyban, S. & Ranov, T. (1970) Mechanism of slug formation in horizontal two- phase flow. *Journal of*
620 *Basic Engineering*. 92 (4), 857–864.

- 621 Lin, P. Y. & Hanratty, T. J. (1987) Detection of slug flow from pressure measurements. *International*
622 *Journal of Multiphase Flow*. [Online] 13 (1), 13–21. [online]. Available from:
623 <http://www.sciencedirect.com/science/article/pii/0301932287900036> (Accessed 14 August 2014).
- 624 Lin, P. Y. & Hanratty, T. J. (1986) Prediction of the initiation of slugs with linear stability theory.
625 *International Journal of Multiphase Flow*. 1279–98.
- 626 Losi, G. et al. (2016) Modelling and statistical analysis of high viscosity oil / air slug flow characteristics
627 in a small diameter horizontal pipe. *Chemical Engineering Science*. [Online] 148190–202. [online].
628 Available from: <http://dx.doi.org/10.1016/j.ces.2016.04.005>.
- 629 Nadler, M. & Mewes, D. (1995) Effects of The Liquid Viscosity on The Phase Distributions in Horizontal
630 Gas-Liquid Slug Flow. *International Journal of Multiphase Flow*. 21 (2), 253–266.
- 631 Nicholson, M. K. et al. (1978) Intermittent two phase flow in horizontal pipes: Predictive models. *The*
632 *Canadian Journal of Chemical Engineering*. [Online] 56 (6), 653–663. [online]. Available from:
633 <http://dx.doi.org/10.1002/cjce.5450560601>.
- 634 Norris, L. (1982) *Correlation of Prudhoe Bay Liquid Slug Lengths and Holdups During Including 1981*
635 *Large Diameter Flowline Tests*.
- 636 Nydal, O. J. et al. (1992) Statistical characterization of slug flow in horizontal pipes. *International*
637 *Journal of Multiphase Flow*. [Online] 18 (3), 439–453. [online]. Available from:
638 <http://www.sciencedirect.com/science/article/pii/030193229290027E> (Accessed 8 August 2015).
- 639 Okezue, C. (2013) Application of the gamma radiation method in analysing the effect of liquid viscosity
640 and flow variables on slug frequency in high viscosity oil-gas horizontal flow. *WIT Transactions on*
641 *Engineering Sciences*. [Online] 79447–461.
- 642 Ouyang, L. & Aziz, K. (2000) A homogeneous model for gas–liquid flow in horizontal wells. *Journal of*
643 *Petroleum Science and Engineering*. 27119–128.
- 644 Pan, J. (2010) *Gas Entrainment in Two-Phase Gas-Liquid Slug Flow*. PhD Thesis thesis. Imperial
645 College London.
- 646 Prestine, C. (2016) *Big Oil Geopolitics 104: Global Oil Reserves – Maps, Charts, Graphs* [online].
647 Available from: <http://www.ogandt.com/2016/02/> (Accessed 1 January 2017).
- 648 Romero, C. H. et al. (2012) ‘Experimental Determination of Hydrodynamic Parameters of Air-Water
649 Two-Phase Slug Flow in Horizontal Pipes’, in *Proceedings of the ASME 2012 Fluids Engineering*
650 *Summer Meeting*. 2012 Rio Grande, Puerto Rico, USA.; ASME. p.
- 651 Santim, C. G. S. et al. (2017) A Transient Analysis of Gas-Liquid Slug Flow Inside a Horizontal Pipe
652 Using Different Models. *Journal of Petroleum Science and Engineering*. [Online] [online]. Available
653 from: <http://linkinghub.elsevier.com/retrieve/pii/S0920410516306234>.
- 654 Scott, S. L. et al. (1989) Prediction of Slug Length in Horizontal, Large-Diameter Pipes. *Society of*
655 *Petroleum Engineers*. [Online] 4 (3), .
- 656 Taitel, Y. and Dukler, A. E. (1976) A model for predicting flow regime transitions in horizontal and near
657 horizontal gas liquid flow. *AIChE Journal*. Vol.2247–55.
- 658 Taitel, Y. et al. (1980) Modelling flow pattern transitions for steady upward gas-liquid flow in vertical
659 tubes. *AIChE Journal*. [Online] 26 (3), 345–354. [online]. Available from:
660 <http://doi.wiley.com/10.1002/aic.690260304> (Accessed 19 May 2013).
- 661 Taitel, Y. & Barnea, D. (1990) A consistent approach for calculating pressure drop in inclined slug flow.
662 *Chemical Engineering Science*. [Online] 45 (5), 1199–1206. [online]. Available from:
663 <http://www.sciencedirect.com/science/article/pii/0009250990871137> (Accessed 19 October 2015).
- 664 Taitel, Y. & Dukler, A. E. (1976) A model for predicting flow regime transitions in horizontal and near
665 horizontal gas-liquid flow. *AIChE Journal*. [Online] 22 (1), 47–55. [online]. Available from:
666 <http://onlinelibrary.wiley.com/doi/10.1002/aic.690220105/abstract>.
- 667 Thaker, J. & Banerjee, J. (2015) Characterization of two-phase slug flow sub-regimes using flow
668 visualization. *Journal of Petroleum Science and Engineering*. [Online] 135561–576. [online].
669 Available from: <http://www.sciencedirect.com/science/article/pii/S0920410515301443> (Accessed

- 670 27 March 2016).
- 671 Ujang, P. M. et al. (2006) *Slug initiation and evolution in two-phase horizontal flow. International Journal*
672 *of Multiphase Flow* [Online] 32 (5); 527-552.
- 673 Wallis, G. B. & Dodson, J. E. (1973) The onset of slugging in horizontal stratified air-water flow.
674 *International Journal of Multiphase Flow.* [Online] 1 (1), 173–193. [online]. Available from:
675 <http://www.sciencedirect.com/science/article/pii/0301932273900104> (Accessed 10 May 2016).
- 676 Wang, S. (2012) *Experiments and Model Development For High-Viscosity Oil / Water / Gas Horizontal*
677 *And Upward Vertical Pipe Flows.* University of Tulsa.
- 678 Weisman, J. et al. (1979) Effects of Fluid Properties and Pipe Diameter on Two-Phase Flow Patterns in
679 Horizontal Line. *International Journal of Multiphase Flow.* 5 (C), 437–462.
- 680 Woods, B. D. et al. (2006) Frequency and development of slugs in a horizontal pipe at large liquid flows.
681 *International Journal of Multiphase Flow.* [Online] 32 (8), 902–925. [online]. Available from:
682 <http://www.sciencedirect.com/science/article/pii/S0301932206000528> (Accessed 25 March 2014).
- 683 Xin, W. et al. (2006) Development of Liquid Slug Length in Gas-Liquid Slug Flow along Horizontal
684 Pipeline: Experiment and Simulation. *Chinese Journal of Chemical Engineering.* [Online] 14 (5),
685 626–633. [online]. Available from:
686 <http://www.sciencedirect.com/science/article/pii/S1004954106601250> (Accessed 1 September
687 2015).
- 688 Zhao, Y. (2014) *High Viscosity Liquid Two-phase Flow.* PhD Thesis thesis. United Kingdom: Cranfield
689 University, United Kingdom.
- 690 Zhao, Y. (2014) *High Viscosity Liquid Two-phase Flow.* Ph.D thesis. United Kingdom: Cranfield
691 University.
- 692 Zhao, Y. et al. (2015) Investigation and prediction of slug flow characteristics in highly viscous liquid
693 and gas flows in horizontal pipes. *Chemical Engineering Research and Design.* [Online] 102124–
694 137. [online]. Available from:
695 <http://www.sciencedirect.com/science/article/pii/S0263876215002075> (Accessed 29 August 2015).
- 696
- 697

Table 1: Summary of experimental studies high viscosity oil-gas flow

Author(s)	Liquid		Gas		Pipe			Parameters Measured	Models/Correlations Proposed
	Type	Viscosity (cP)	Density (kg/m ³)	Type	ID (m)	Inclination (Degree)	Material		
Abdulkadir et al., 2016	Oil	525	900	Air	0.067	0	Acrylic	Flow pattern, slug frequency, holdup, slug velocity, lengths of liquid slug and elongated bubble, pressure gradient	N/A
Archibong (2015)	Oil	1000- 7500	916	Air	0.0762, 0.0254	0, 30	Acrylic	Flow pattern, slug frequency, holdup, slug velocity	Distribution parameter, slug liquid holdup, Slug Frequency
Al-Safran et al., (2013)	Oil	587	-	Air	0.0508	0	Acrylic	Slug Frequency	Slug Frequency
Al-Safran et al.,(2005, 2011, 2013)	Oil	181-587	-	Air	0.0508	0	Acrylic	Slug length	Slug Length
Brito et al., (2013)	Oil	10-180	-	-	0.0508	-	-	Pressure gradient, flow pattern, translational velocity	-
Farsetti et al, (2014)	Oil	900	-	Air	0.0228	0, 5, 10, 15, -5, -15	NA	Pressure Gradient Slug Frequency Slug Holdup	NA
Foletti et al., 2011	Oil	896	886	Air	0.022	0	Plexiglas	Pressure Gradient	NA
Gokcal et al., (2010)	Oil	181-590	-	Air	0.0508	0	NA	-	Slug Frequency
Gokcal et al. (2006)	Oil	181-590	-	-	0.022	0	NA	Flow pattern	NA
Gokcal (2008)	Oil	181-590	-	-	0.0508	0	NA	Flow pattern, slug frequency, holdup, slug velocity, drift velocity and slug length	Slug frequency
Kora et al., 2011	Oil	181, 257, 387, 587	-	Air	0.0508	0	Acrylic	Slug Liquid Holdup	Slug Liquid Holdup
Nadler & Mewes (1995)	Oil	14-37	-	Air	0.059	0	-	Liquid holdup	-
Schulkes, 2011	Oil	1-590	-	Air	0.019 – 0.1	0 - 80	-	-	Slug Frequency

Weisman et al., 1986	glycerol-water	75, 150	-	Air	0.012, 0.051	0.025, 0	-	Flow pattern	NA
Wang, 2012	Oil	15, 28, 57	890	air	0.0508	0, 90	NA	Slug liquid holdup and mean slug length	Slug liquid holdup and mean slug length
Zhao et al., 2013	Oil	1000, 3500	916	Air	0.0762	0	Acrylic	Slug Frequency	Slug Frequency

Table 2: Summary of measured slug length by some researchers

Authors	Measured average slug length
(Dukler and Hubbard, 1975)	Ls = 30D
(Nicholson et al., 1978)	Ls = 15-27D
(Barnea and Brauner, 1985)	Ls = 15-40D
(Nydal et al., 1992)	Ls = 12-30D
(He, 2002)	Ls = 10-34D
(Xin et al., 2006)	Ls = 15-27D
(Pan, 2010)	Ls = 24D
(Al-safran et al., 2011)	Ls = 10D
Present Study	Ls = 6D

Table 3: Summary of existing correlations in the literature for slug length

Authors/ Year	Experimental conditions/ Data Source	Correlations developed for slug frequency	Comments
(Heywood and Richardson, 1978)	-	$L_S = \frac{V_m(1 + V_T)}{f_s} \frac{H_L - H_F}{H_S - H_F}$	Correlation developed based on observation using Air-Water as test fluids
(Brill et al., 1981)	Alaska Prudhoe Bay field data	$\ln(L_S) = -3.851 + 0.059 \ln\left(\frac{V_m}{0.3048}\right) + 5.445 \left[\ln\left(\frac{D}{0.0254}\right) \right]^{0.5}$	Correlation only accounted for few parameters (i.e. Mixture velocity and pipe diameter) and was developed based on observation using Air and light oil as test fluids
(Norris, 1982)	Modified (Brill et al., 1981)	$\ln\left(\frac{L_S}{0.3048}\right) = -2.099 + 4.859 \sqrt{\ln\frac{D}{0.0254}}$	Simply carried out a modification of the (Brill et al., 1981) correlation and accounted for just pipe diameter.
(Gordon and Fairhurst, 1987)	ID = 0.3048 m, 0.4064 m and 0.508 m	$\ln L_S = -3.287 + 4.859 \sqrt{\ln D + 3.673} + 0.059 \ln(V_m)$	This correlation accounted for just pipe diameter and mixture velocity and mixture velocity
(Gordon and Fairhurst, 1987)	ID = 0.3048 m, 0.4064 m and 0.508 m and 0.588 m	$\ln L_S = -3.287 + 4.859 \sqrt{\ln D + 3.673}$	More data points were utilized for this correlation though accounted for only pipe diameter.
(Scott et al., 1989)	Alaska Prudhoe Bay field data	$\ln L_S = -26.6 + 28.495 \left[\ln\left(\frac{D}{0.0254}\right) \right]^{0.1}$	Correlation valid for very large diameter pipe data
(Wang, 2012)	0.0525 m ID pipe, 0.15 to 0.57 Pa.s.	$L_S = \left\{ 10.1 + \frac{16.8}{1 + \exp[-3.57 * (\ln(N_f) - 5.4)]} \left[\cos^2 \theta + \frac{\sin^2 2\theta}{2} \right] D \right\}$	Experimental data was sourced from observation using light oil of less than 0.1 Pa.s
(Al-safran et al., 2011)	Air-oil; ID=0.0508 m, 0.181 – 0.589 Pa. s	$\frac{L_S}{D} = 2.63 \left[\frac{D^{2/3} \sqrt{\rho_L(\rho_L - \rho_G)}}{\mu_L} \right]^{0.321}$	Accounted for viscosity effects however, only medium oil viscosities were used.
(Losi et al., 2016)	Air-oil; ID = 0.022 m, 0.037 -0.804 Pa s; $j_L = 0.1-0.3$ m/s and $j_g = 1.3 - 2.2$ m/s	$\frac{L_S}{D} = A \left[j_g + \frac{j_{go}^2}{j_g} \right]$ where j_g is the superficial gas velocity corresponding to the minimum slug length and the constant A is a function of liquid properties (details in Losi et al., 2016) while j_{go} is the critical superficial gas velocity	Also accounted for viscosity effects but experiment were conducted in a small diameter pipe.

Table 4: Summary of existing models for onset slugging criterion

Authors/ Year	Onset slugging criterion	Comments
(Wallis and Dodson, 1973)	$V_g - V_l \geq K \left\{ \frac{g(\rho_L - \rho_G)h_G}{\rho_G} \right\}^{\frac{1}{2}}$	Based on an experimental and analytical study of transition to slug flow in essentially horizontal rectangular channels geometry with small amplitude waves. K experimentally determined to be 0.5
(Taitel, Y. and Dukler, 1976)	$V_g - V_l \geq K \left\{ \frac{g(\rho_L - \rho_G)h_G}{\rho_G} \right\}^{\frac{1}{2}}$ Can be approximated to $J_{GL} = \alpha^{2.5}$	The growth of a finite disturbance on a smooth stratified layer in a horizontal channel was considered. For an infinitesimal disturbance, the value of K will be unity due to the overestimation. Hence (Taitel, Y. and Dukler, 1976) recommended $K = \left\{ 1 - \frac{h_l}{D} \right\}$. The model was observed to work reasonably for horizontal small diameter pipes using air-water flows at atmospheric pressure.
(Mishima and Ishii, 1980)	$V_g - V_l \geq K \left\{ \frac{g(\rho_L - \rho_G)h_G}{\rho_G} \right\}^{\frac{1}{2}}$	(Mishima and Ishii, 1980) obtained K to be 0.487 by extension of the stability theory of finite-amplitude interfacial waves as proposed by (Kordyban and Ranov, 1970). This model suits the prediction of transition to slug flow in a rectangular duct well.
(Lin and Hanratty, 1986)	$V_g = K \left\{ \frac{gD(\rho_L - \rho_G)h_G}{\rho_G} \right\}^{\frac{1}{2}}$	The application of linear stability theory was explored to explain the onset of slugging. A Good agreement was established between the linear stability analysis and observations of the initiation of slugs in horizontal pipes. K was taken to be $f(\alpha, V_m, V_{sg})$
(Anoda et al., 1989)	$V_g \geq K \left\{ \frac{g(\rho_L - \rho_G)h_G}{\rho_G dA_L/dh_L} \right\}^{\frac{1}{2}}$ Where $K = \left\{ 1 - \frac{h_l}{D} \right\}$,	A modified form of (Taitel, Y. and Dukler, 1976)
(Barnea and Taitel, 1994)	$(V_G \geq V_L)$ $< K \left\{ (\rho_L \alpha - \rho_G \varepsilon) \frac{\rho_L - \rho_G}{\rho_L \rho_G} g \cos \theta \frac{A}{dA_L/dh_L} \right\}^{\frac{1}{2}}$ $K_V = \left\{ 1 - \frac{(C_{IV} - C_V)^2}{\frac{\rho_L - \rho_G}{\rho_L \rho_G} g \cos \theta \frac{A}{dA_L/dh_L}} \right\}^{1/2}$ $C_{IV} = \frac{\rho_L V_{SL} \alpha + \rho_L V_{SG} \varepsilon}{\rho_L \alpha + \rho_L \varepsilon}$ $C_V = \frac{\left[\frac{\partial F}{\partial \varepsilon} \right]_{V_{sl}, V_{sg}}}{\left[\frac{\partial F}{\partial V_T} \right]_{V_{sl}, \varepsilon} - \left[\frac{\partial F}{\partial V_T} \right]_{V_{sl}, \varepsilon}}$	Considered a long wavelength interfacial instabilities and their growth. For inviscid flow $K=1$, for viscous case $K=K_V$

	$F = -\frac{\tau_{lf}S_l}{A_l} + \frac{\tau_{gf}S_g}{A_g} + \tau_i S_i \left(\frac{1}{A_l} + \frac{1}{A_g} \right) - (\rho_L - \rho_G)g \sin\theta$	
(Hideo, 1996)	$V_g \geq K \left\{ \frac{g(\rho_L - \rho_G)h_G}{\rho_G dA_l/dh_l} \right\}^{\frac{1}{2}}$ <p>Where $K = \left\{ 1 - \frac{h_l}{D} \right\}^n$</p>	Modified the coefficient (K) value of the (Taitel, Y. and Dukler, 1976) model. This model is best suited for relatively-low pressure flows in large-diameter pipes with n=2
(Chun et al., 1995)	$V_g \geq K \left\{ \frac{g(\rho_L - \rho_G)h_G}{\rho_G} \right\}^{\frac{1}{2}}$	A theoretical relationship developed for the wave height in a stratified wavy flow regime using the concept of total energy balance over a wave crest considering the shear stress acting on the interface of two fluids. K was found to be 0.470
(Chang-Kyung and Moon-Hyun, 1996)	$V_g = \left(1 - \frac{h_l}{D} \right) \left\{ \frac{\pi \Delta \rho \alpha g D \cos\theta}{4 \sin\gamma} K \right\}^{\frac{1}{2}}$	A more general expression for the onset of slug criterion derived from singular points and neutral stability conditions of the transient 1-D equations of two fluid model presented. K was given as $1 + \frac{\alpha \rho_g}{\rho_L \varepsilon}$

Table 5: Experimental test matrix and fluid properties

S/N	Density (kg/m ³)	Test fluids	Viscosity (cP)	Interfacial tension (25°C, N/m)	Test matrix (m/s)	API gravity
1	1.293	Air	0.017	0.033	0.3-9.0	-
2	≈ 1000	Water	1	0.029	0.06-0.4	-
3	≈ 918	CYL680	1000~6000	0.033	0.06-0.3	22.67

Table 6: Uncertainties in measurements

Measurements	Uncertainty (%)
Superficial liquid velocity	±0.5
Superficial gas velocity	±2.1
Liquid viscosity	± 1
Pressure drop	± 2
Liquid holdup	± 5

Table 5: Snapshots of observed flow patterns

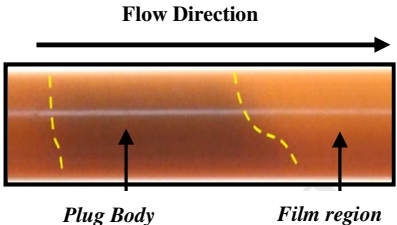
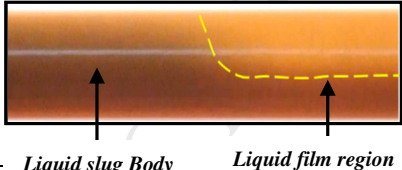
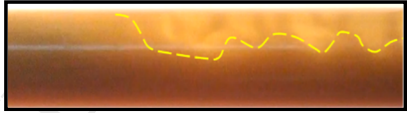
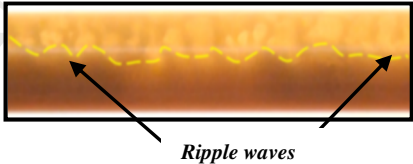
Nomenclature	Flow Condition	Video image
Plug Flow	V_{SL} 0.3m/s, V_{SG} 0.3-0.7m/s	
Slug Flow	V_{SL} 0.3m/s, V_{SG} 0.7-3.0 m/s	
Pseudo Slug Flow	V_{SL} 0.3m/s V_{SG} 3.0-5.0 m/s	
Wavy Annular Flow	V_{SL} 0.3m/s, V_{SG} 5.0-9.0 m/s	

Table 8: Statistical evaluation of surveyed slug length correlations

	Proposed Correlation	Brill (1981)	Norris (1982)	Scott (1989)	Wang (2012)	Al-Safran et al, (2013)
ϵ_1	0.517391	-34.1318	7401.188	10088.98	181.3125	14.4496
ϵ_2	8.468193	46.13764	7401.188	10088.98	181.3125	20.30533
ϵ_3	10.6204	34.29429	1238.391	1888.901	104.2071	18.50914
ϵ_4	-0.15192	-4.55236	761.5418	1061.032	16.29675	2.736121
ϵ_5	1.505312	5.205357	761.5418	1061.032	16.29675	2.09782
ϵ_6	1.892089	3.638863	165.4363	295.3714	2.976471	2.064682

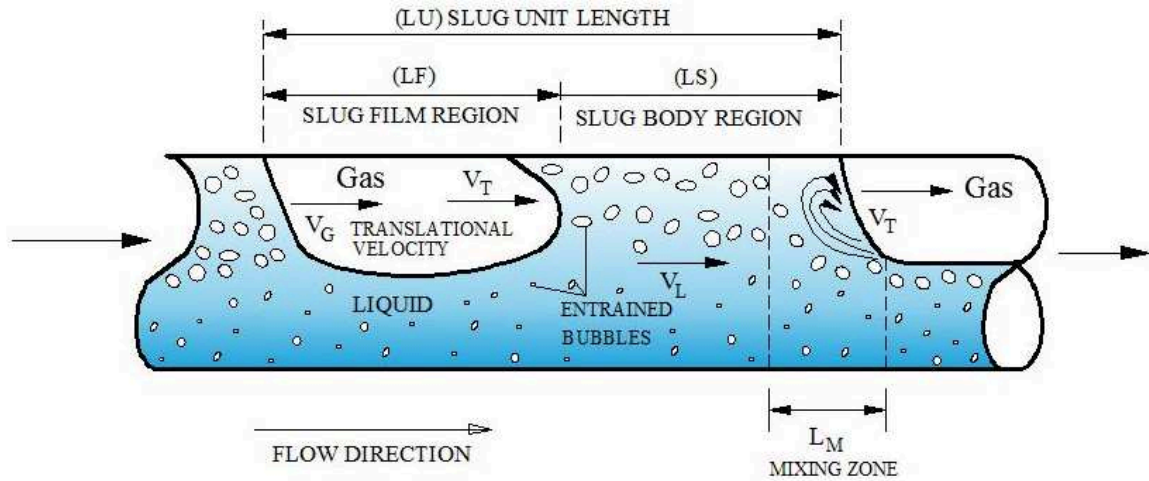


Figure 1: Slug Flow Geometry (Baba, 2016)

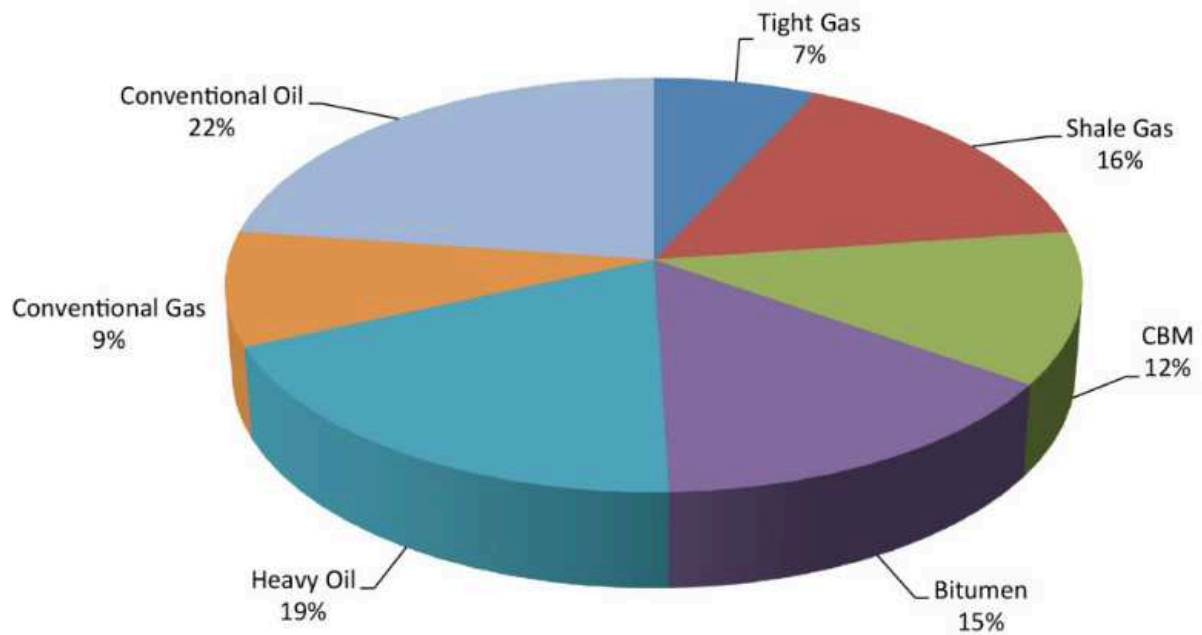


Figure 2: Global oil reserves -conventional versus unconventional resources (Prestine, 2016)

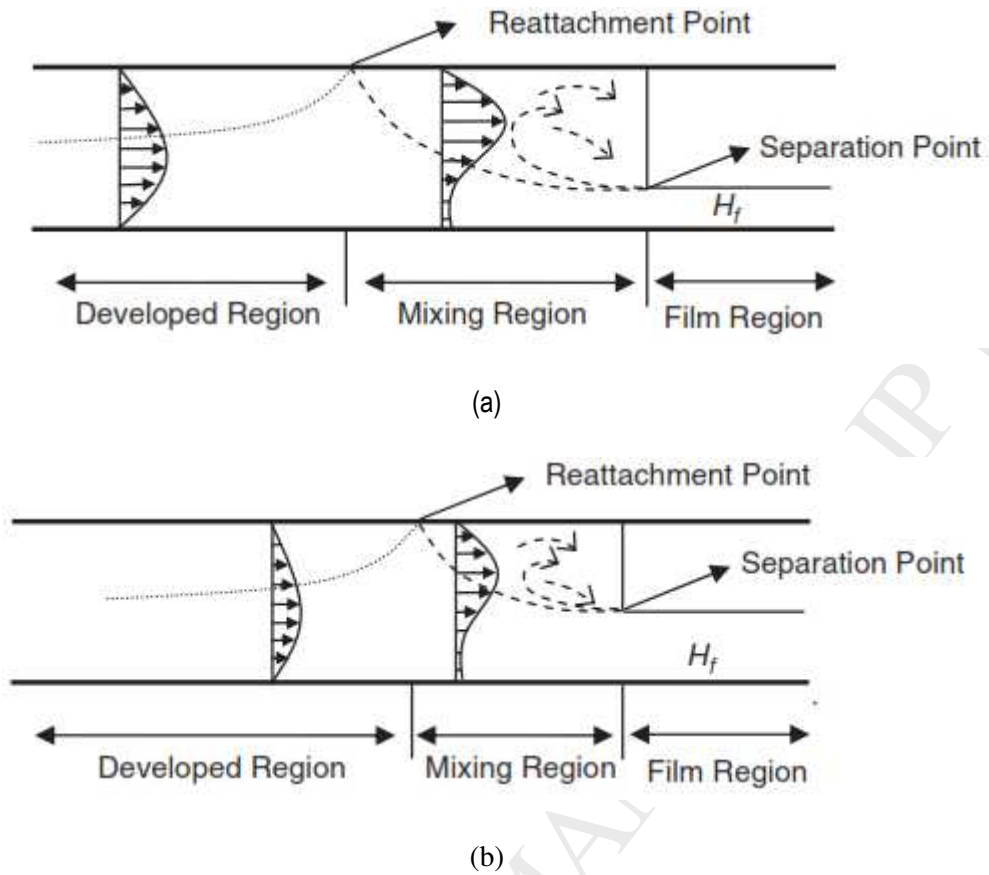


Figure 3: (a) Physical model minimum slug length in light oil, (Dukler and Hubbard, 1975) (b) physical model minimum slug length in high viscosity oil, (Al-safran et al., 2013)

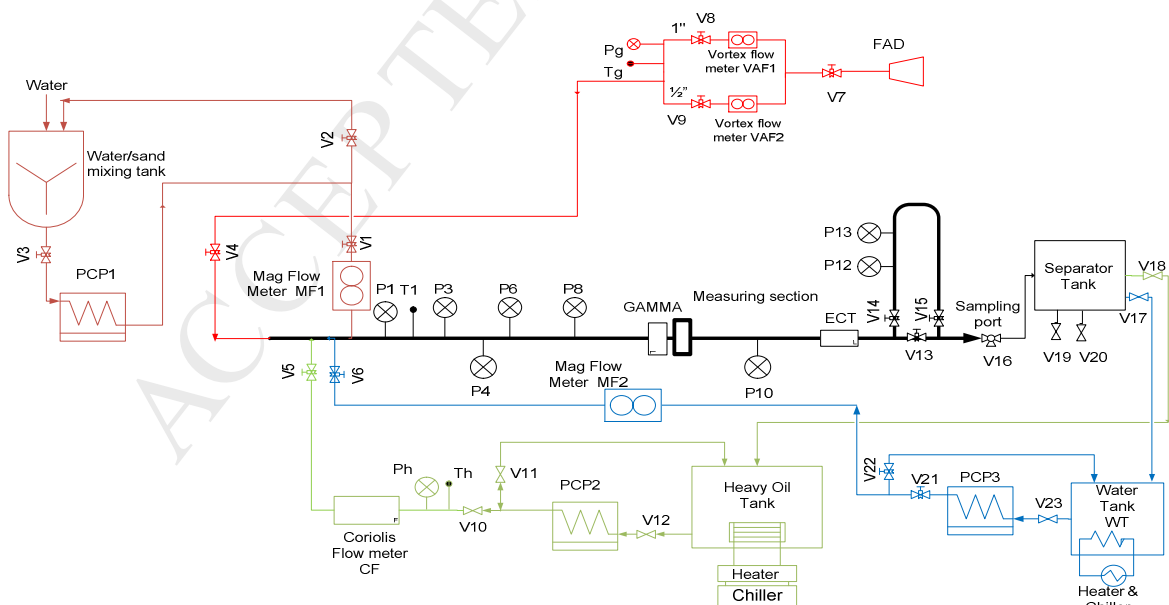


Figure 4: Schematic of experimental test facility.

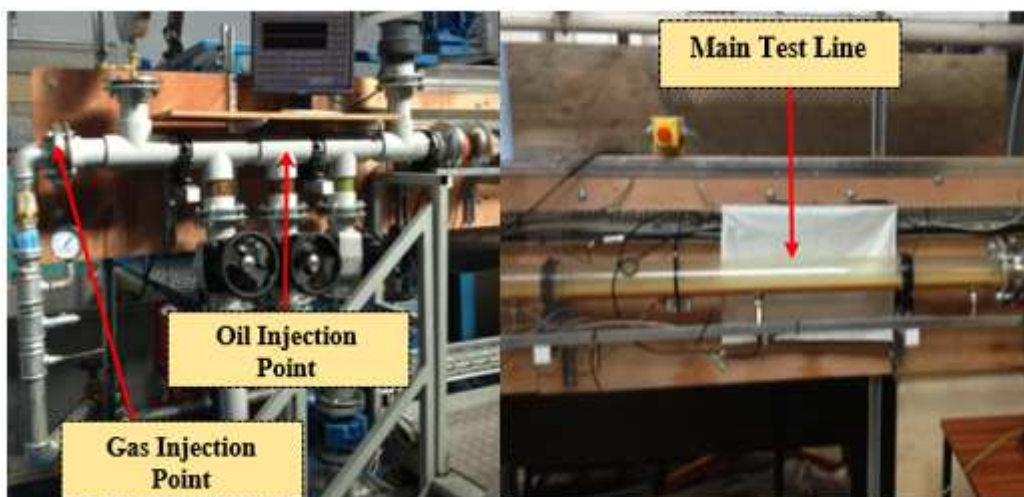


Figure 5: Pictorial view of test facility injection point.

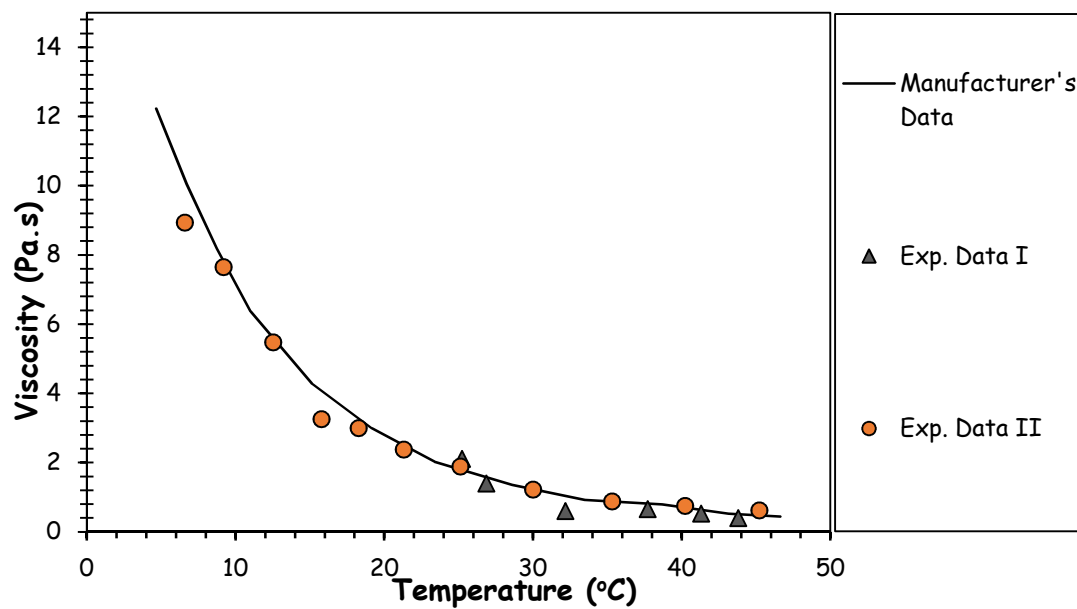


Figure 6: Comparison of measured viscosity and manufacturer's data

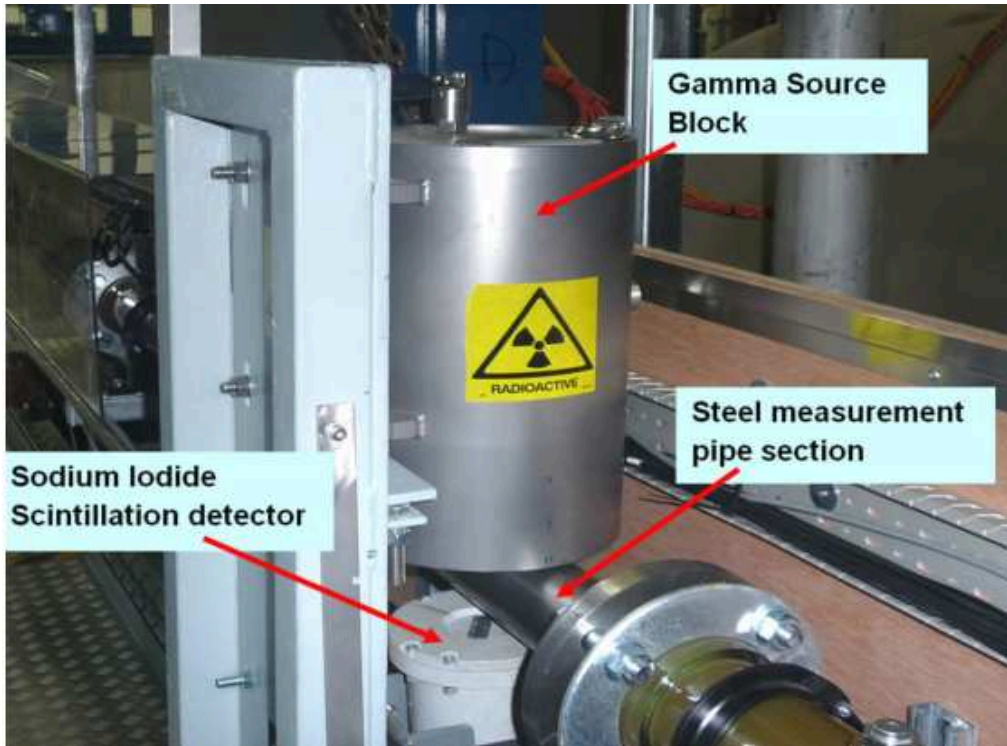


Figure 7: Pictorial representation of gamma ray densitometer used as instrumentation

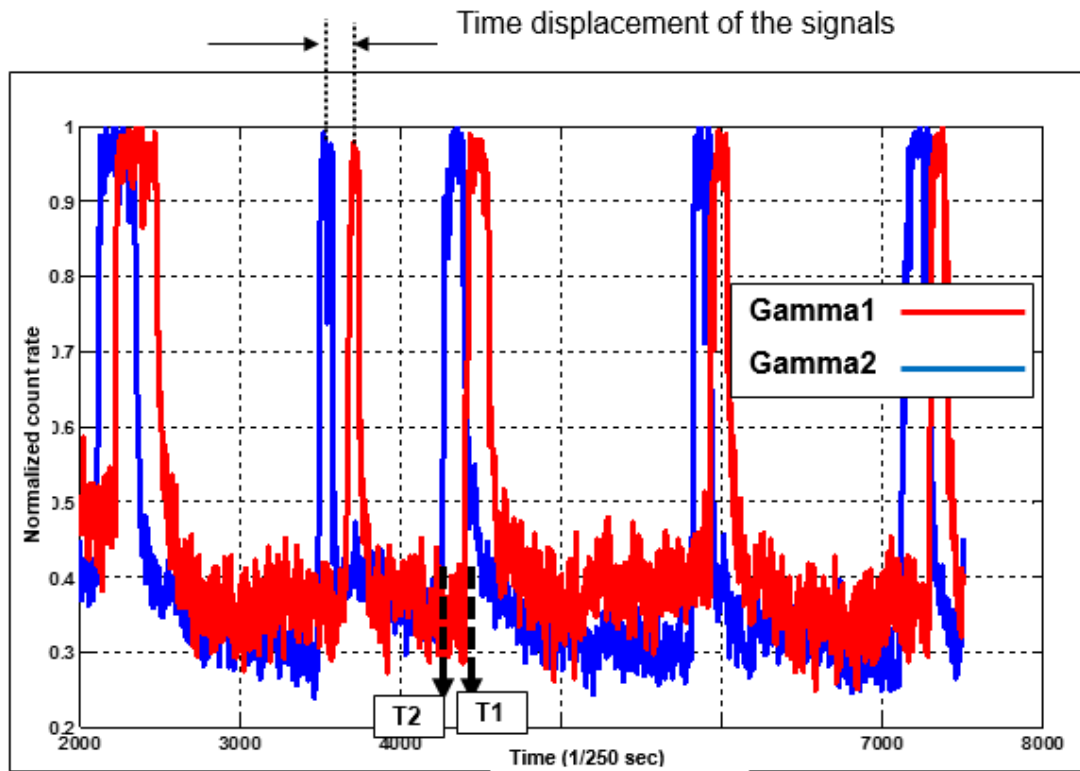


Figure 8: A typical gamma densitometer time series liquid holdup plot for dual Gamma Sensor

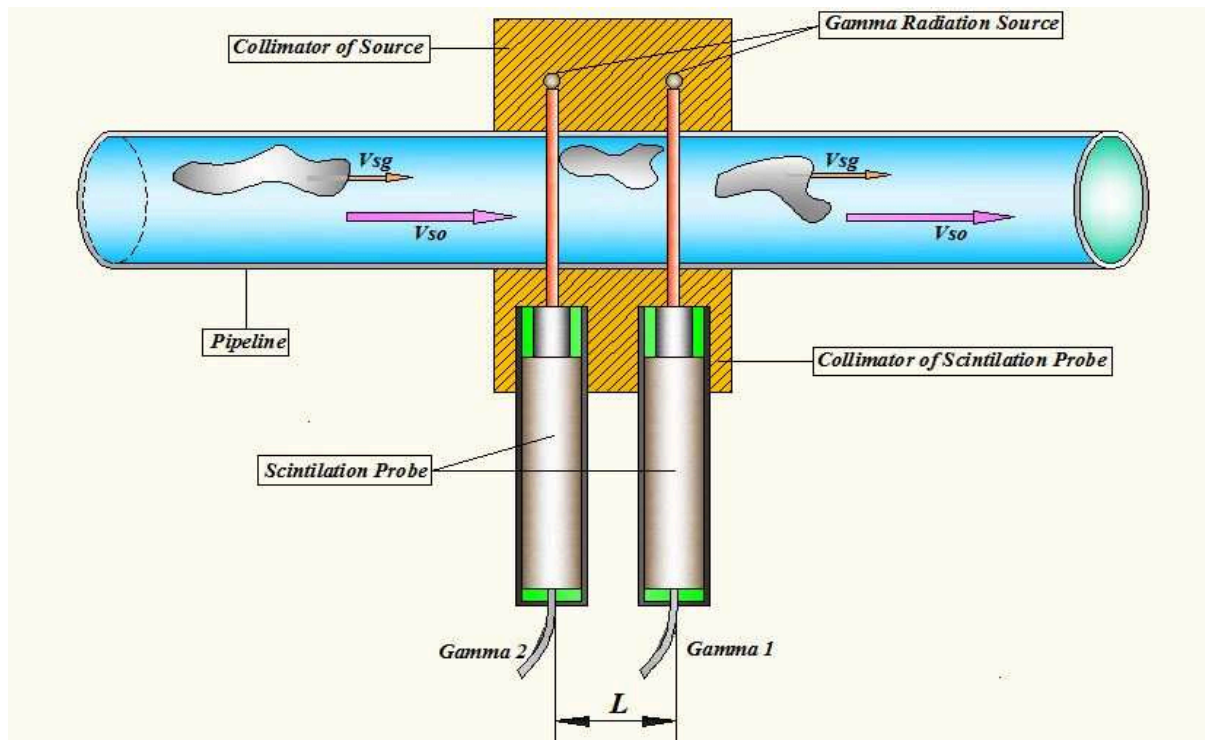
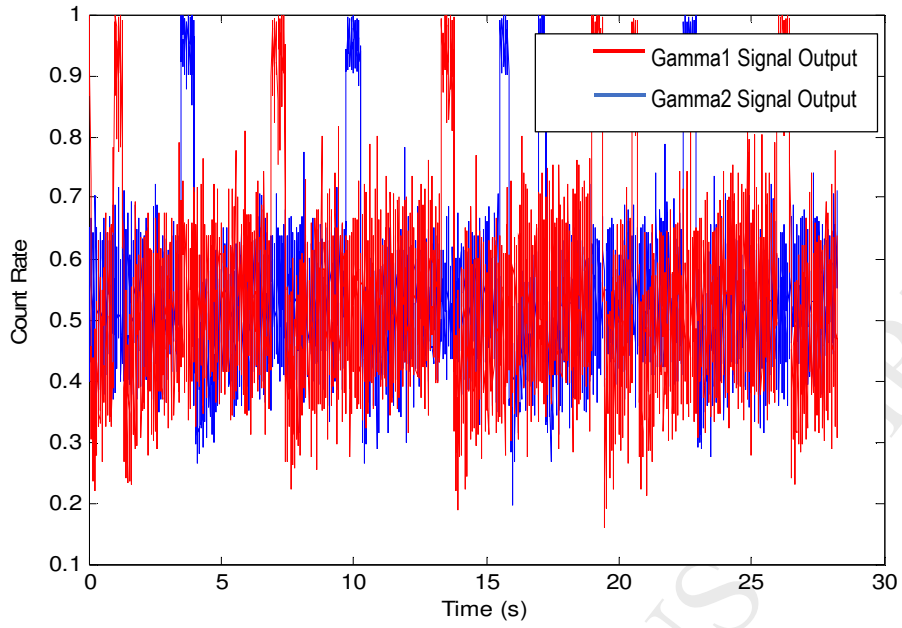
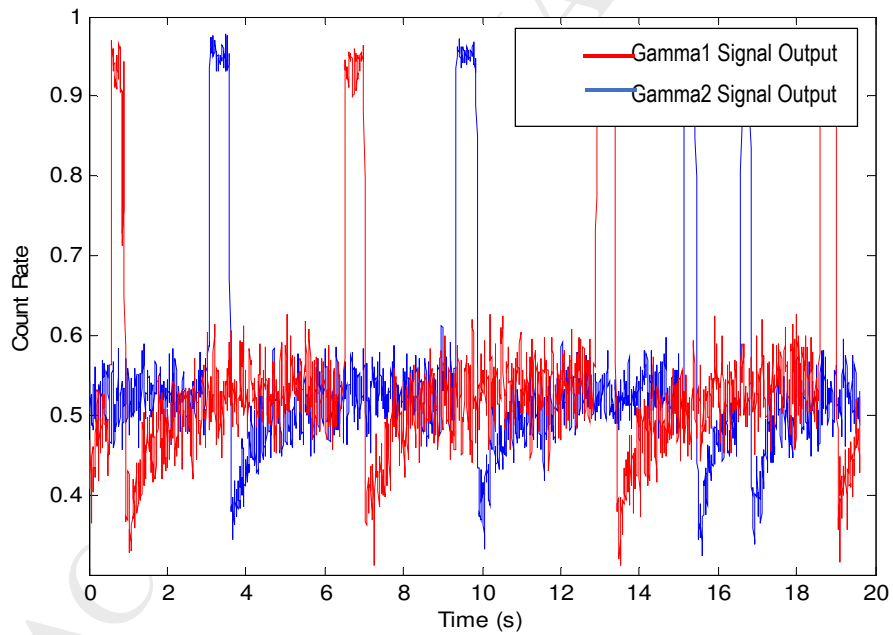


Figure 9: Diagrammatic representation of the Gamma Source installed on the test facility.



(a)



(b)

Figure10: (a) Raw signal output from gamma photon counts. (b) Sample of a filtered signal output.

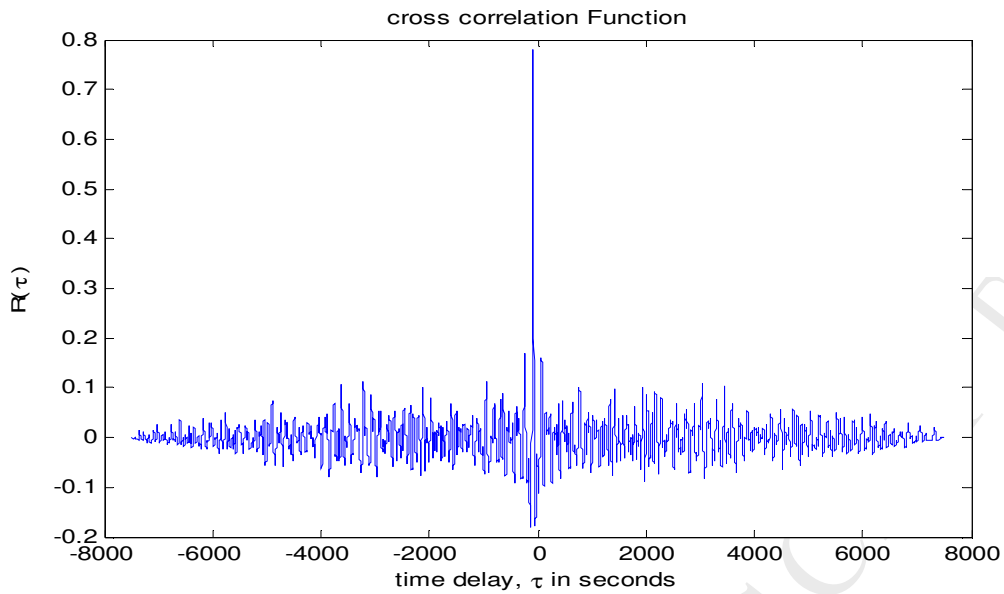
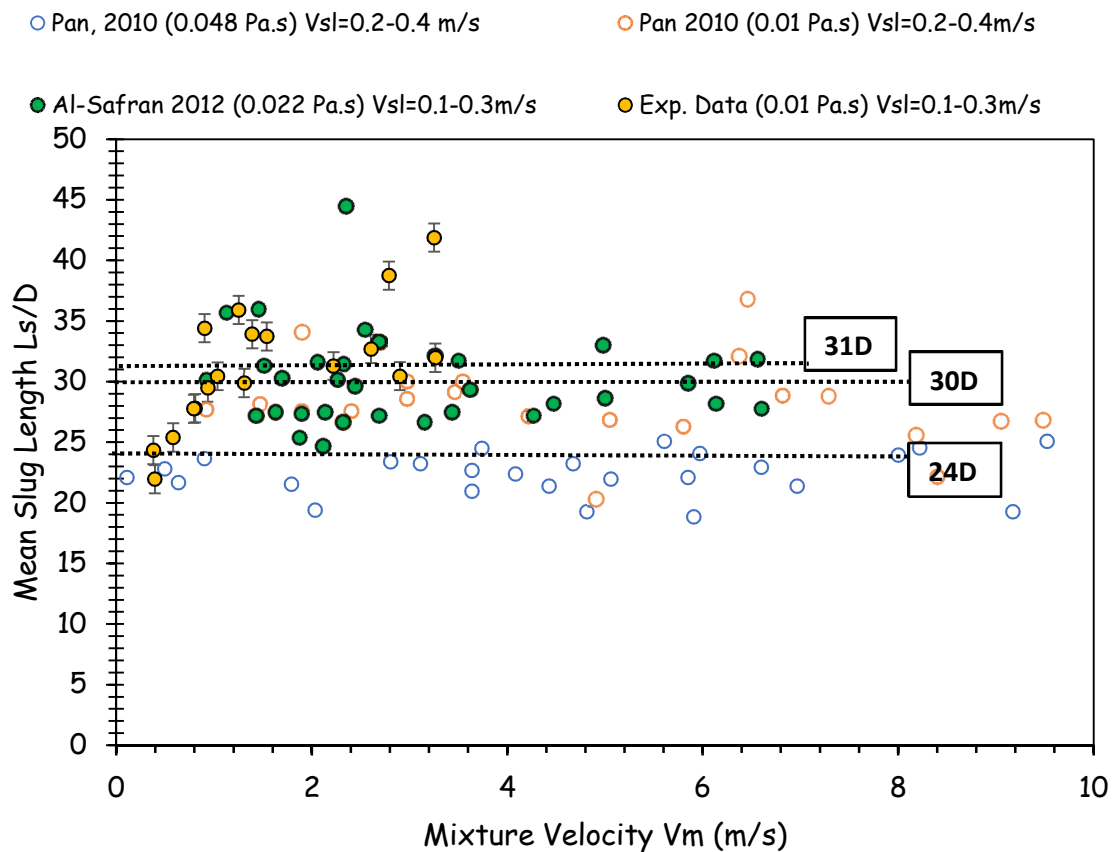
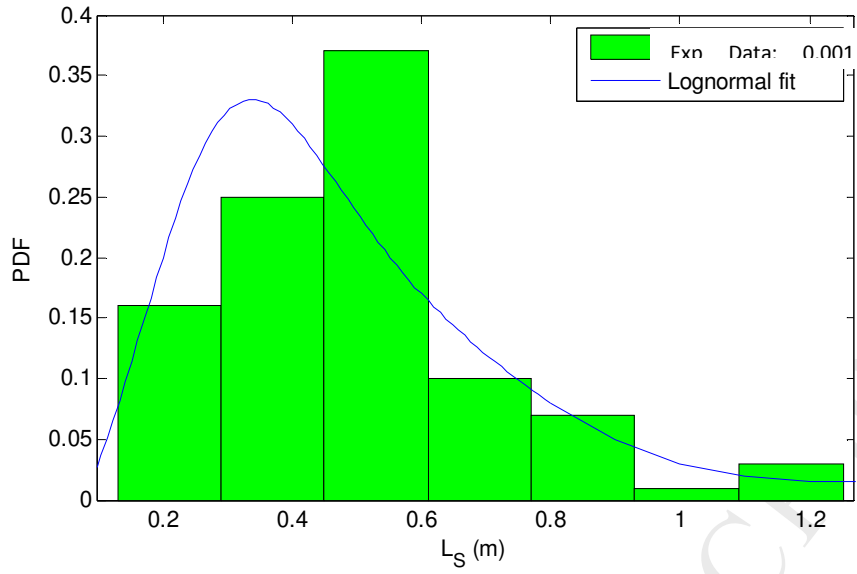


Figure 11: Cross-Correlation results between Gamma 1 and Gamma 2.

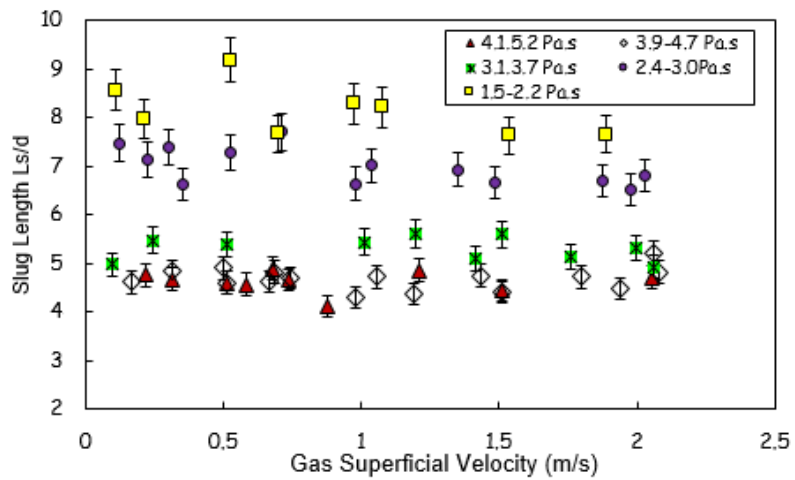


(a)

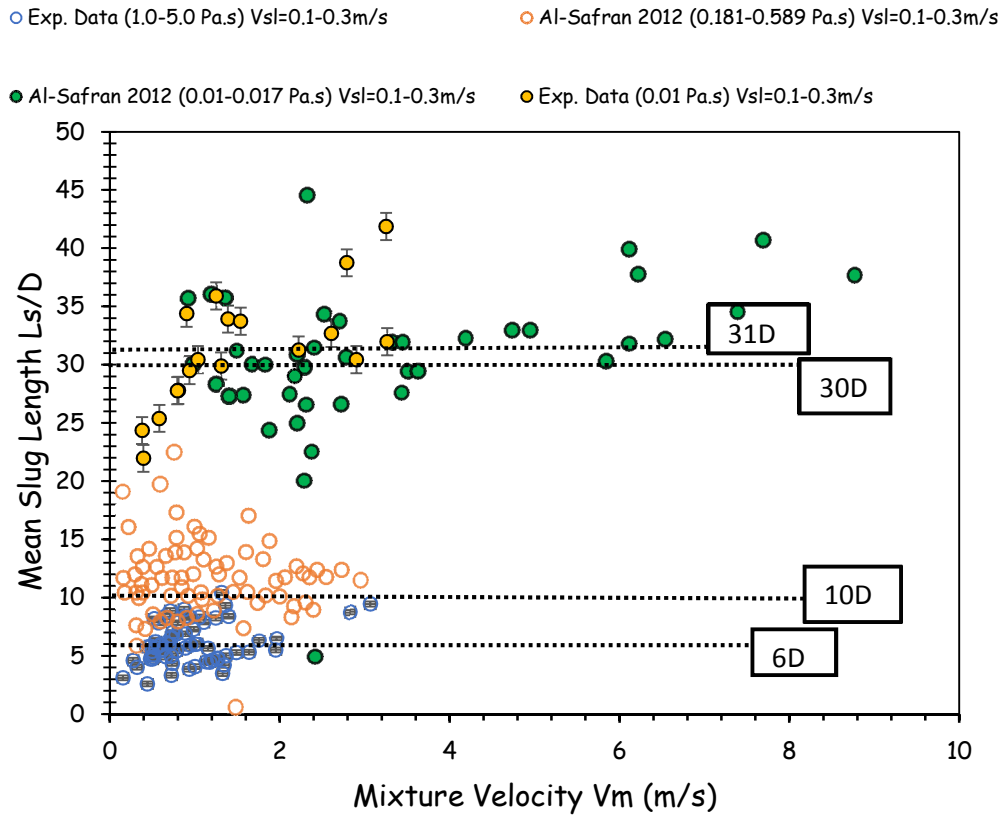


(b)

Figure 12: (a) Measured slug length as a function of mixture velocity (b) Slug length distribution and log-normal fit for flow conditions investigated ($V_{sg}=0.3-7\text{m/s}$ and $V_{sl}=0.2-0.4\text{m/s}$)



(a)



(b)

Figure 13: (a) Measured slug length versus superficial gas velocity for different superficial liquid velocity $V_{sl}=0.06-0.3\text{m/s}$. (b) Mean Slug Length as a Function of Mixture Velocity. Error bars were calculated from the uncertainty equation (i.e. Eq. 12) given in Appendix.

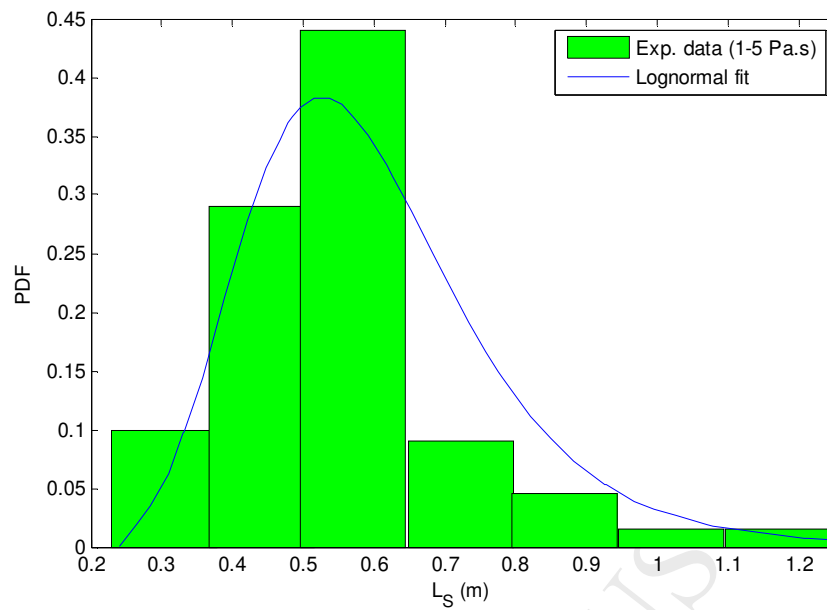


Figure 14: Comparison of experimental result for slug length and Log-Normal distribution.

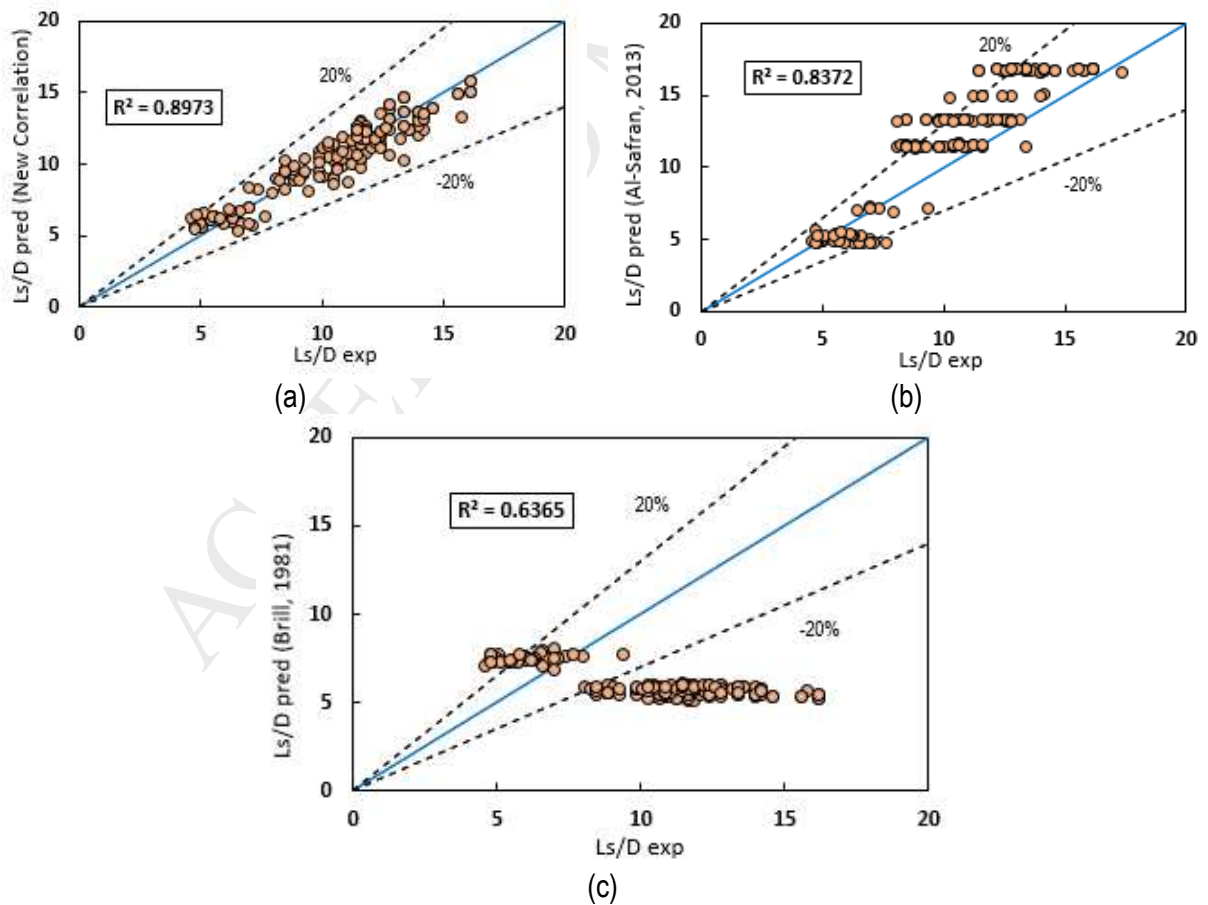


Figure 15: Cross-plot of predictive model predictions for best performing correlations against experimental measurement (a) Current (b) Al Safran (2013) (c) Brill (1981)

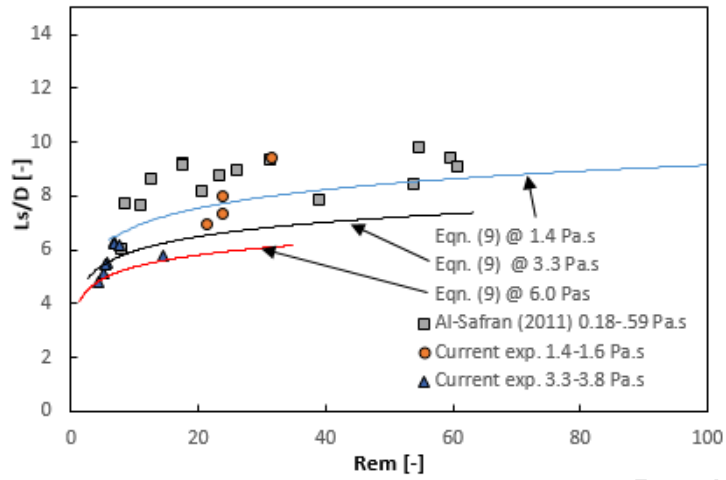


Figure 16: Use of Al-Safran (2013) and current experimental data concerned with oil viscosities ranging from 0.18–6.00 Pa.s to validate Eqn. (9)

Highlights

- High viscosity Liquid-Gas-liquid two-phase flow experiments were conducted in a large diameter horizontal pipe.
- Unique measurements of slug flow features using fast sampling Gamma Densitometer
- Oil viscosity far higher than those found in the literature was used owing to its increasing relevance to the industry.
- Performance evaluation of existing prediction models was carried out against present data
- A new correlation for slug length in high viscosity liquid proposed